

PAPER

## Blind ptychography: uniqueness and ambiguities

To cite this article: Albert Fannjiang and Pengwen Chen 2020 *Inverse Problems* **36** 045005

View the [article online](#) for updates and enhancements.



**IOP | ebooks**<sup>TM</sup>

Bringing you innovative digital publishing with leading voices to create your essential collection of books in STEM research.

Start exploring the [collection](#) - download the first chapter of every title for free.

# Blind ptychography: uniqueness and ambiguities

Albert Fannjiang<sup>1,3</sup>  and Pengwen Chen<sup>2</sup> 

<sup>1</sup> Department of Mathematics, University of California, Davis, CA 95616, United States of America

<sup>2</sup> Applied Mathematics, National Chung Hsing University, Taichung 402, Taiwan, Republic of China

E-mail: [fannjiang@math.ucdavis.edu](mailto:fannjiang@math.ucdavis.edu) and [pengwen@nchu.edu.tw](mailto:pengwen@nchu.edu.tw)

Received 5 September 2019, revised 3 December 2019

Accepted for publication 23 December 2019

Published 26 February 2020



CrossMark

## Abstract

Ptychography with an unknown mask and object is analyzed for general ptychographic measurement schemes that are strongly connected and possess an anchor.

Under a mild constraint on the mask phase, it is proved that the masked object estimate must be the product of a block phase factor and the true masked object. This local uniqueness manifests itself in the phase drift equation that determines the ambiguity at different locations connected by ptychographic shifts.

The proposed mixing schemes effectively connects the ambiguity throughout the whole domain such that a distinct ambiguity profile arises and consequently possess the global uniqueness that the block phases have an affine profile and that the object and mask can be simultaneously recovered up to a constant scaling factor and an affine phase factor.

Keywords: phase retrieval, ptychography, uniqueness, ambiguity

(Some figures may appear in colour only in the online journal)

## 1. Introduction

Ptychography is the scanning version of coherent diffractive imaging (CDI) [6] that acquires multiple diffraction patterns through the scan of a localized illumination on an extended object (figure 1). The redundant information in the overlap between adjacent illuminated spots is then exploited to improve phase retrieval methods [39, 43, 45]. Ptychography originated in electron microscopy [19, 25, 26, 29, 37, 38, 44] and has been successfully implemented with x-ray, optical

<sup>3</sup> Author to whom any correspondence should be addressed.

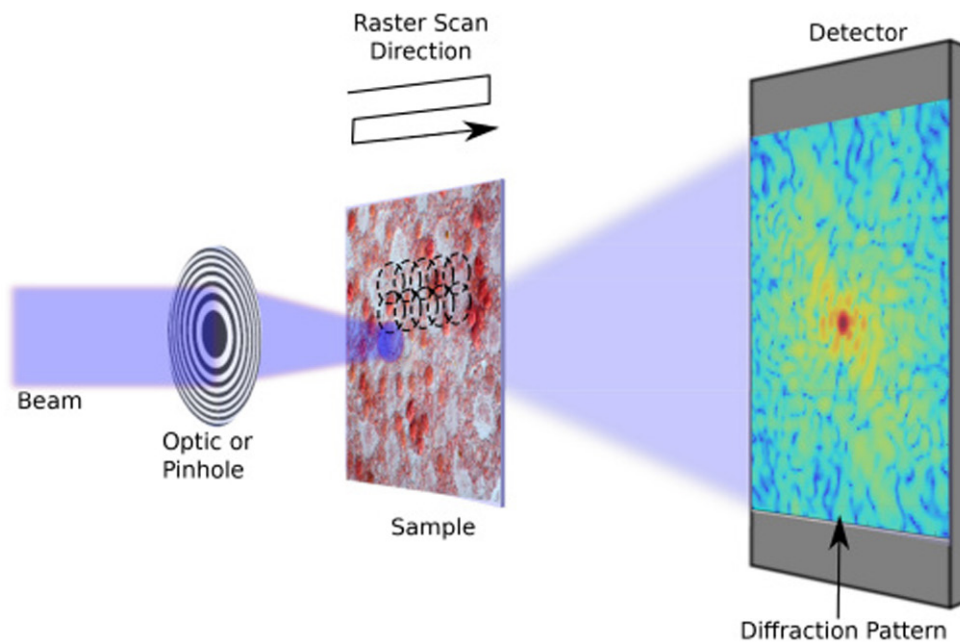


**Figure 1.** Simplified ptychographic setup showing a Cartesian grid used for the overlapping raster scan positions. Adapted with permission from [36] © The Optical Society.

and terahertz waves [8, 18, 46, 48, 51, 52, 54]. Recently ptychography has been extended to the Fourier domain [40, 41, 60]. In Fourier ptychography, illumination angles are scanned sequentially with a programmable array source with the diffraction pattern measured at each angle.

Ptychographic CDI has its origin in a concept developed for the crystallographic phase problem: Hoppe [25] pointed out that if one can make the Bragg peaks of crystalline diffraction patterns interfere, information about their relative phases can be obtained and therefore suggested to use a localized illumination instead of the usual extended plane wave. Due to the Fourier convolution theorem, the crystal's diffraction peaks in the resulting far-field pattern are then convolved with the Fourier transform of the localized illumination. When the extent of the illumination is shrunk to about the same order of magnitude as the crystalline unit cell, this leads to overlap between adjacent Bragg peaks and thus the desired interferences. While these interferences already allow to determine the relative phases, the twin-image ambiguity remains. Hoppe showed that an unambiguous result can be obtained by recording another diffraction pattern at a slightly shifted position of the localized illumination. Hoppe [26] further discussed the extension of ptychography to non-periodic objects and the possibility of scanning transmission electron diffraction microscopy.

An important development in ptychography since the work of Thibault *et al* [51, 52] is the potential of simultaneous recovery of the object and the illumination (blind ptychography). Blind ptychographic reconstruction is affected by many factors such as the type of illumination and the amount of overlap between adjacent illuminations. In practice, numerical reconstruction with the widely used algorithm, the extended ptychographic iterative engine (ePIE), and its variants typically require 60%–70% overlap between adjacent illuminations [5, 31, 33] (see section 9 for more discussion). The convergence of numerical reconstruction is monitored with the residual of the ptychographic data or the difference between successive estimates [20, 23, 33, 34, 52, 53, 56].

Even in the noiseless case, however, numerical convergence does not necessarily imply recovery of the mask and the object. To ensure that a vanishing residual (data fitting) implies a vanishing reconstruction error in the noiseless case, we need a theory of uniqueness of solution. To be sure, a completely blind ptychography or phase retrieval is untenable.

First of all, even with a complete prior information of the mask/illumination, we have shown in a recent work [7] that twin-image ambiguity does arise if the Fresnel number of the commonly used Fresnel illumination takes on certain values, resulting in poor reconstruction and hinting on the benefits of avoiding symmetry and increasing complexity of the mask. A simple way to avoid symmetry and increase complexity is to use a random mask for illumination. Random masking is a form of coded aperture and has found applications in many imaging modalities and significant improvements on imaging qualities [1, 2, 4, 7, 10, 11, 15, 21, 27, 28, 30, 31, 32, 42, 47, 49, 50, 55, 57–59].

For nonptychographic phase retrieval, the capability of a randomly coded aperture in removing all the ambiguities, including the translation and twin-image ambiguities, was rigorously analyzed in [12]. Moreover, uniqueness theory for blind phase retrieval with a plain and a randomly coded diffraction pattern has been developed in [16] which assumes slight prior knowledge about the phase range of the random mask. In other words, with a plain and a randomly coded diffraction pattern one can uniquely and simultaneously determine both the unknown object and the unknown mask. In contrast, in blind ptychography we work with just one unknown mask which is more challenging. As random masks are typically harder to calibrate (but easier to fabricate) than a deterministic mask, blind ptychography and phase retrieval is particularly useful when a random mask is used.

This paper concerns the uniqueness question for blind ptychography with a randomly phased mask under certain prior information. We exhibit examples to show these priors are in some sense necessary. Moreover, we aim to characterize a general class of measurement schemes that avoid the pitfalls of the regular raster scan shown in figure 1 (see examples 6.4 and 6.5).

### 1.1. Inherent ambiguities

Let us begin with two inherent ambiguities to blind ptychography.

Let  $\llbracket k, l \rrbracket$  denote the integers between and including the integers  $k$  and  $l$ . Let  $\mathcal{M}^0 := \mathbb{Z}_m^2 = \llbracket 0, m-1 \rrbracket^2$  be the initial window area, i.e. the support of the mask  $\mu^0$ . Let  $\mathcal{M}$  be the object domain containing the support of the discrete object  $f$ .

Let  $\mathcal{T}$  be the set of all shifts, including  $(0, 0)$ , involved in the ptychographic measurement. Denote by  $\mu^{\mathbf{t}}$  the  $\mathbf{t}$ -shifted probe for all  $\mathbf{t} \in \mathcal{T}$  and  $\mathcal{M}^{\mathbf{t}}$  the domain of  $\mu^{\mathbf{t}}$ . Let  $f^{\mathbf{t}}$  the object restricted to  $\mathcal{M}^{\mathbf{t}}$ . We refer to each  $f^{\mathbf{t}}$  as a part of  $f$  and write  $f = \vee_{\mathbf{t}} f^{\mathbf{t}}$  where  $\vee$  is the ‘union’ of functions consistent over their common support set. In ptychography, the original object is broken up into a set of overlapping object parts, each of which produces a  $\mu^{\mathbf{t}}$ -coded diffraction pattern. The totality of the coded diffraction patterns is called the ptychographic measurement data. Let  $\nu^0$  (with  $\mathbf{t} = (0, 0)$ ) and  $g = \vee_{\mathbf{t}} g^{\mathbf{t}}$  be any pair of the probe and the object estimates producing the same ptychography data as  $\mu^0$  and  $f$ , i.e. the diffraction pattern of  $\nu^{\mathbf{t}} \odot g^{\mathbf{t}}$  is identical to that of  $\mu^{\mathbf{t}} \odot f^{\mathbf{t}}$  where  $\nu^{\mathbf{t}}$  is the  $\mathbf{t}$ -shift of  $\nu^0$  and  $g^{\mathbf{t}}$  is the restriction of  $g$  to  $\mathcal{M}^{\mathbf{t}}$ . For simplicity, we assume the periodic boundary condition on  $\mathcal{M}$  (i.e. discrete torus). The periodic boundary condition refers to the measurement scheme when the mask crosses over the boundaries of the object domain  $\mathcal{M}$  and should not be taken as the assumption of  $f$  being a periodic object. The latter implies the former but not vice versa.

Consider the probe and object estimates

$$\nu^0(\mathbf{n}) = \mu^0(\mathbf{n}) \exp(-ia - i\mathbf{r} \cdot \mathbf{n}), \quad \mathbf{n} \in \mathcal{M}^0 \quad (1)$$

$$g(\mathbf{n}) = f(\mathbf{n}) \exp(ib + i\mathbf{r} \cdot \mathbf{n}), \quad \mathbf{n} \in \mathcal{M} \quad (2)$$

for any  $a, b \in \mathbb{R}$  and  $\mathbf{r} \in \mathbb{R}^2$ . For any  $\mathbf{t}$ , we have the following calculation

$$\begin{aligned} \nu^{\mathbf{t}}(\mathbf{n}) &= \nu^0(\mathbf{n} - \mathbf{t}) \\ &= \mu^0(\mathbf{n} - \mathbf{t}) \exp(-i\mathbf{r} \cdot (\mathbf{n} - \mathbf{t})) \exp(-ia) \\ &= \mu^{\mathbf{t}}(\mathbf{n}) \exp(-i\mathbf{r} \cdot (\mathbf{n} - \mathbf{t})) \exp(-ia) \end{aligned}$$

and hence for all  $\mathbf{n} \in \mathcal{M}^{\mathbf{t}}, \mathbf{t} \in \mathcal{T}$

$$\nu^{\mathbf{t}}(\mathbf{n})g^{\mathbf{t}}(\mathbf{n}) = \mu^{\mathbf{t}}(\mathbf{n})f^{\mathbf{t}}(\mathbf{n}) \exp(i(b - a)) \exp(i\mathbf{r} \cdot \mathbf{t}). \quad (3)$$

Since for each  $\mathbf{t}$ ,  $\nu^{\mathbf{t}} \odot g^{\mathbf{t}}$  is the phase factor  $\exp(i(b - a)) \exp(i\mathbf{r} \cdot \mathbf{t})$  times  $\mu^{\mathbf{t}} \odot f^{\mathbf{t}}$  where  $\odot$  is the entry-wise (Hadamard) product,  $g$  and  $\nu^0$  produce the same ptychographic data as  $f$  and  $\mu^0$ . This holds true regardless of the set  $\mathcal{T}$  of shifts and the mask.

In addition to the affine phase ambiguity (1) and (2), a scaling factor ( $g = cf, \nu^0 = c^{-1}\mu^0, c > 0$ ) is inherent to any blind ptychography. However, when the mask is exactly known (i.e.  $\nu^0 = \mu^0$  up to a constant phase factor),  $\mathbf{r} = \mathbf{0}$  and  $c = 1$  so neither ambiguity can occur.

In addition, for the regular raster scan (figure 1), it is well known that blind ptychography is susceptible to many other artifacts [51]. For a complete analysis of these ambiguities, the reader is referred to [13].

A crucial question then is, Under what conditions are the scaling factor and the affine phase ambiguity the only ambiguities in blind ptychography? We aim to answer this question in this paper.

Briefly and informally, we summarize the results as follows.

## 1.2. Contributions

The first basic requirement of our method is the strong connectivity property of the object with respect to the measurement scheme. It is useful to think of connectivity in graph-theoretical terms (figure 2): let the ptychographic experiment be represented by a complete graph  $\Gamma$  whose nodes correspond to  $\{f^{\mathbf{t}} : \mathbf{t} \in \mathcal{T}\}$ . Given any positive integer  $s$ , an edge between two nodes corresponding to  $f^{\mathbf{t}}$  and  $f^{\mathbf{t}'}$  is  $s$ -connective if

$$|\mathcal{M}^{\mathbf{t}} \cap \mathcal{M}^{\mathbf{t}'} \cap \text{supp}(f)| \geq s \quad (4)$$

where  $|\cdot|$  denotes the cardinality. In the case of full support (i.e.  $\text{supp}(f) = \mathcal{M}$ ), (4) becomes  $|\mathcal{M}^{\mathbf{t}} \cap \mathcal{M}^{\mathbf{t}'}| \geq s$ . An  $s$ -connective reduced graph  $\Gamma_s$  of  $\Gamma$  consists of all the nodes of  $\Gamma$  but only the  $s$ -connective edges. Two nodes are adjacent (and neighbors) in  $\Gamma_s$  iff they are  $s$ -connected. A chain in  $\Gamma_s$  is a sequence of nodes such that two successive nodes are adjacent. In a simple chain all the nodes are distinct. Then the object parts  $\{f^{\mathbf{t}} : \mathbf{t} \in \mathcal{T}\}$  are  $s$ -connected if and only if  $\Gamma_s$  is a connected graph, i.e. every two nodes is connected by a chain of  $s$ -connective edges. Loosely speaking, an object is strongly connected w.r.t. the ptychographic scheme if  $s \gg 1$ .

The second requirement is the existence of an *anchoring* part. Informally speaking, an object part  $f^{\mathbf{t}}$  is an anchor if its support touches four sides of  $\mathcal{M}^{\mathbf{t}}$  (figure 3). Specifically, an object part  $f^{\mathbf{t}}$  is an anchor if  $f^{\mathbf{t}}$  has a tight support in  $\mathcal{M}^{\mathbf{t}}$ , i.e.

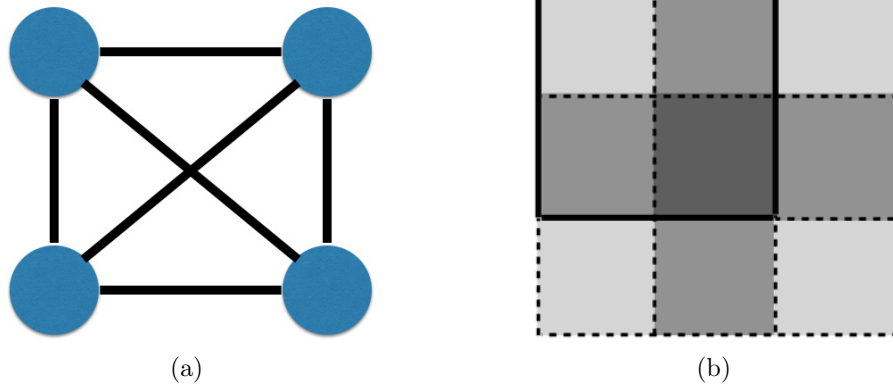


**Figure 2.** A complete undirected graph (a) representing four connected object parts (b) where the grey level indicates the number of coverages by the mask in four scan positions.

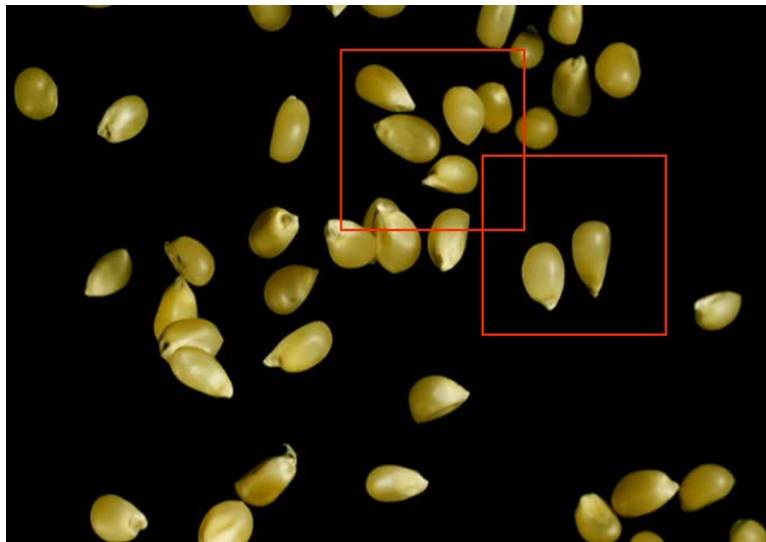


**Figure 3.** Sparse objects such as this image of corn grains, where the dark area represents zero pixel value, can be challenging to ptychographic measurements. The two red-framed blocks are not connected even though they overlap. The object part in the lower-right block is not an anchor since the object support does not touch the four sides of the block while the object part in the upper-left block is an anchor. Indeed, the two corn grains at the lower-left and upper-right corners alone of the latter block suffice to create a tight support.

$$\text{Box}[\text{supp}(\mathbf{f}^t)] = \mathcal{M}^t \tag{5}$$

where  $\text{Box}[\mathbf{E}]$  stands for the box hull, the smallest rectangle containing  $E$  with sides parallel to  $\mathbf{e}_1 = (1, 0)$  or  $\mathbf{e}_2 = (0, 1)$ . An object part does not have a tight support if and only if it has a loose support. Clearly,  $f^t$  has a tight support if and only if  $\text{Twin}(\mathbf{f}^t)$  does since  $\text{Box}[\text{supp}(\mathbf{f}^t)] = \text{Box}[\text{supp}(\text{Twin}(\mathbf{f}^t))] + \mathbf{m}$  for some  $\mathbf{m}$ . In the case  $\text{supp}(f) = \mathcal{M}$ , any

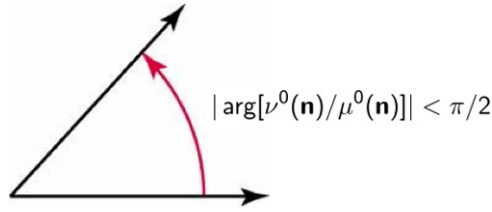


**Figure 4.**  $\nu^0$  satisfies MPC if  $\nu_0(\mathbf{n})$  and  $\mu^0(\mathbf{n})$  form an acute angle for all  $\mathbf{n}$ .

object part is an anchor. For an extremely sparse object such as shown in figure 3, the anchoring assumption can pose a challenge.

For the unknown mask, we need some prior information called the *mask phase constraint* (MPC):

*The mask estimate  $\nu^0$  has the property  $\Re(\bar{\nu}^0 \odot \mu^0) > 0$  at every pixel (where  $\odot$  denotes the component-wise product and the bar denotes the complex conjugate).*

See figure 4. MPC can be relaxed as  $|\arg[\nu^0(\mathbf{n})/\mu^0(\mathbf{n})]| < \pi/2$  for *sufficiently large percentage* of  $\mathbf{n}$ . For simplicity of presentation, however, we shall work with the technically simplifying version as above.

Even with the perfect knowledge of the mask amplitude, MPC allows a large relative error

$$\sqrt{\frac{1}{\pi} \int_{-\pi/2}^{\pi/2} |e^{i\phi} - 1|^2 d\phi} = \sqrt{2(1 - \frac{2}{\pi})} \approx 0.8525$$

when  $\arg[\nu^0]$  is selected randomly and uniformly in the interval  $|\arg[\nu^0(\mathbf{n})/\mu^0(\mathbf{n})]| < \pi/2$ .

For any strongly connective scheme under the assumptions of MPC and anchoring, we prove the local uniqueness result for blind ptychography (theorems 3.1 and 3.3) that with high probability (exponentially close to 1 in  $s$ ) in the random selection of  $\mu^0$ ,

$$\nu^{\mathbf{t}} \odot g^{\mathbf{t}} = e^{i\theta_{\mathbf{t}}} \mu^{\mathbf{t}} \odot f^{\mathbf{t}}, \quad \mathbf{t} \in \mathcal{T}, \quad (6)$$

for some constants  $\theta_{\mathbf{t}} \in \mathbb{R}$  (called block phases) if  $g$  and  $\nu^{\mathbf{t}}$  produce the same diffraction pattern as  $f$  and  $\mu^{\mathbf{t}}$  for all  $\mathbf{t} \in \mathcal{T}$ . As shown by examples 4.1 and 4.2, both MPC and the anchoring assumption are in some sense necessary for (6) to hold.

We refer to the ambiguity equation (6) as the *local uniqueness* property since  $\theta_{\mathbf{t}}$  may be more complicated than just an affine profile,  $\theta_0 + \mathbf{t} \cdot \mathbf{r}$ , for some  $\mathbf{r} \in \mathbb{R}^2$ , as in (3). Indeed, the affine phase ambiguity (1) and (2) means that the relation (6) with an affine profile in  $\theta_{\mathbf{t}}$  is the best to hope for. On the other hand, we say that the *global uniqueness* holds if the affine phase ambiguity and the scaling factor ambiguity are the only ambiguities. We say that a ptychographic scheme is *complete* for a given object if the global uniqueness holds.

The ambiguity equation (6) can be transformed into the phase drift equation which plays the key role in our theory. Consider the object ambiguity represented by

$$h(\mathbf{n}) \equiv \ln g(\mathbf{n}) - \ln f(\mathbf{n}), \quad \forall \mathbf{n} \in \mathcal{M},$$

provided that both  $f$  and  $g$  are non-vanishing. The phase drift equation

$$h(\mathbf{n} + \mathbf{t}) - h(\mathbf{n} + \mathbf{t}') = i\theta_{\mathbf{t}} - i\theta_{\mathbf{t}'} \pmod{2\pi}, \quad \forall \mathbf{n} \in \mathcal{M}^0, \quad \forall \mathbf{t}, \mathbf{t}' \in \mathcal{T} \quad (7)$$

equates the difference in the object ambiguity in different blocks with the phase drift in the block phase.

Most important, we show that the mixing schemes, introduced here for the first time, ‘mix’ the ambiguity so completely that a distinct ambiguity profile (affine phase plus scaling factor) arises and the global uniqueness holds true (theorem 8.3). The mixing schemes include the special case of small perturbations of the regular raster scan (theorems 7.4 and 7.5). On the other hand, while the global uniqueness fails for the regular raster scan, the block phases nevertheless have an affine profile (proposition 6.1).

The rest of the paper is organized as follows. In section 2, we formulate the basic building block of the ptychographic measurement and discuss ambiguities in standard phase retrieval with one coded diffraction pattern. In section 3 we consider the ptychography with two overlapping diffraction patterns and prove the local uniqueness for the masked object (theorem 3.1). We then extend the local uniqueness to the multi-part ptychography (theorem 3.3). In section 4 we demonstrate with examples that the prior information of MPC and anchoring is necessary for the local uniqueness result (examples 4.1 and 4.2). In section 5, we develop the phase drift equation that holds the key to the global uniqueness result. In section 6, we exhibit additional ambiguities associated with the regular raster scan (examples 6.4 and 6.5) and prove that the block phases of the raster scan must have an affine profile (proposition 6.1). In section 7, we prove the global uniqueness theorems for the perturbed raster scans with the overlap ratio greater than 50% (theorems 7.4 and 7.5). In section 8, we give an example showing that the minimum overlap ratio 50% is necessary for the perturbed raster scans to be ptychographically complete and introduce the mixing schemes which are ptychographically complete and whose block phases must have an affine profile (theorem 8.3). We conclude in section 9 and discuss a few practical implications of our theory. A preliminary version of this paper was presented in [14].

## 2. Coded diffraction pattern

We start with the set-up of coded diffraction patterns [35].

Let  $f^0$  be a part of the unknown object  $f$  restricted to the initial block  $\mathcal{M}^0 = \mathbb{Z}_m^2$ ,  $m < n$ , and let the Fourier transform of  $f^0$  be written as

$$F(e^{-i2\pi\mathbf{w}}) = \sum_{\mathbf{k} \in \mathcal{M}^0} e^{-i2\pi\mathbf{k} \cdot \mathbf{w}} f^0(\mathbf{k}), \quad \mathbf{w} = (w_1, w_2).$$

Under the Fraunhofer approximation, the diffraction pattern can be written as

$$|F(e^{-i2\pi\mathbf{w}})|^2 = \sum_{\mathbf{k} \in \widetilde{\mathcal{M}}^0} \left\{ \sum_{\mathbf{k}' \in \mathcal{M}^0} f^0(\mathbf{k}' + \mathbf{k}) \overline{f^0(\mathbf{k}')} \right\} e^{-i2\pi\mathbf{k} \cdot \mathbf{w}}, \quad \mathbf{w} \in [0, 1]^2 \quad (8)$$

where

$$\widetilde{\mathcal{M}}^0 = \{(k_1, k_2) \in \mathbb{Z}^2 : -m + 1 \leq k_1 \leq m - 1, -m + 1 \leq k_2 \leq m - 1\}$$

and  $f^0$  assumes the value zero outside of  $\mathcal{M}^0$ . Here and below the over-line notation means complex conjugacy.

The expression in the brackets in (8) is the autocorrelation function of  $f^0$  and the summation over  $\mathbf{n}$  takes the form of Fourier transform on the enlarged grid  $\widetilde{\mathcal{M}}^0$ . Hence sampling  $|F|^2$  on the grid

$$\mathcal{L} = \left\{ (w_1, w_2) \mid w_j = 0, \frac{1}{2m-1}, \frac{2}{2m-1}, \dots, \frac{2m-2}{2m-1} \right\} \quad (9)$$

provides sufficient information to recover the autocorrelation function.

A randomly coded diffraction pattern measured with the mask  $\mu^0$  is the diffraction pattern for the *masked object*  $\tilde{f}^0(\mathbf{n}) = f^0(\mathbf{n})\mu^0(\mathbf{n})$  where the mask function  $\mu^0$  is a finite array of random variables. The masked object is also called the *exit wave* in the parlance of optics literature. In other words, a coded diffraction pattern is just the plain diffraction pattern of a masked object.

We assume randomness in the phases  $\theta$  of the mask function  $\mu^0(\mathbf{n}) = |\mu^0(\mathbf{n})|e^{i\theta(\mathbf{n})}$  where  $\theta(\mathbf{n})$  are independent, continuous real-valued random variables. In other words, each  $\theta(\mathbf{n})$  is independently distributed with a probability density function  $p_\gamma$  supported on  $(-\gamma\pi, \gamma\pi]$  with a constant  $\gamma \in [0, 1]$ . Continuous phase modulation can be experimentally realized with various techniques such as spread spectrum phase modulation [59].

We also require that  $|\mu^0(\mathbf{n})| \neq 0, \forall \mathbf{n} \in \mathcal{M}^0$  (i.e. the mask is transparent). This is necessary for unique reconstruction of the object as any opaque pixels of the mask would block the transmission of the object information.

First we review the case of a plain diffraction pattern ( $\mu^0 \equiv 1$ ).

**Proposition 2.1 ([22]).** *Let the  $z$ -transform  $F(\mathbf{z}) = \sum_{\mathbf{n}} f^0(\mathbf{n})\mathbf{z}^{-\mathbf{n}}$  be given by*

$$F(\mathbf{z}) = \alpha \mathbf{z}^{-\mathbf{m}} \prod_{k=1}^p F_k(\mathbf{z}), \quad \mathbf{m} \in \mathbb{N}^2, \quad \alpha \in \mathbb{C} \quad (10)$$

where  $F_k, k = 1, \dots, p$ , are non-monomial irreducible polynomials. Let  $G(\mathbf{z})$  be the  $\mathbf{z}$ -transform of another finite array  $g^0(\mathbf{n})$ . Suppose  $|F(e^{-i2\pi\mathbf{w}})| = |G(e^{-i2\pi\mathbf{w}})|, \forall \mathbf{w} \in [0, 1]^2$ . Then

$$G(\mathbf{z}) = |\alpha| e^{i\theta} \mathbf{z}^{-\mathbf{p}} \left( \prod_{k \in I} F_k(\mathbf{z}) \right) \left( \prod_{k \in I^c} \overline{F_k(1/\bar{\mathbf{z}})} \right), \quad \text{for some } \mathbf{p} \in \mathbb{N}^2, \theta \in \mathbb{R}, \quad (11)$$

where  $I$  is a subset of  $\{1, 2, \dots, p\}$ .

**Remark 2.2.** The undetermined monomial factor  $\mathbf{z}^{-\mathbf{p}}$  in (11) corresponds to the translation invariance of the Fourier intensity data while the altered factors  $\overline{F_k(1/\bar{\mathbf{z}})}$  corresponds to the conjugate inversion invariance of the Fourier intensity data (see corollary 2.4 below). The conjugate inversion of  $f^0$ , called the twin image, in  $\mathcal{M}^0$  is defined by  $\text{Twin}(\mathbf{f}^0)(\mathbf{n}) = \overline{\mathbf{f}^0(\mathbf{m}, \mathbf{m}) - \mathbf{n}}$ .

Next consider a random mask  $\mu^0$  and assume that  $f^0$  is not a linear object. An object is a linear object if its support is a subset of a line. We recall a result in [12] that the  $z$ -transform of the non-linear masked object  $\tilde{f}^0(\mathbf{n}) = f^0(\mathbf{n})\mu^0(\mathbf{n})$  is irreducible, up to a monomial.

**Proposition 2.3 ([12]).** *Suppose  $f^0$  is not a linear object and let  $\mu^0$  be the phase mask with phase at each point continuously and independently distributed. Then with probability one the  $z$ -transform of the masked object  $\tilde{f}^0 = f^0 \odot \mu^0$  does not have any non-monomial irreducible polynomial factor.*

A similar result can be proved for masks whose phases are discrete random variables by using more advanced tools from algebraic geometry (e.g. [3], proposition 4.1).

The following corollary is what we will need for proving the local uniqueness theorems.

**Corollary 2.4.** *Under the assumptions of proposition 2.3, if another masked object  $\tilde{g}^0 := \nu^0 g^0$  produces the same diffraction pattern as  $\tilde{f}^0 = \mu^0 f^0$ , then for some  $\mathbf{p}$  and  $\theta$*

$$\tilde{f}^0(\mathbf{n} + \mathbf{p}) = e^{-i\theta} \tilde{g}^0(\mathbf{n}) \quad \text{or} \quad e^{i\theta} \text{Twin}(\tilde{g}^0)(\mathbf{n}) \quad (12)$$

for all  $\mathbf{n} \in \mathcal{M}^0$ .

**Proof.** Let  $\tilde{F}$  and  $\tilde{G}$  be the  $z$ -transforms of  $\tilde{f}^0$  and  $\tilde{g}^0$ , respectively. By proposition 2.3 and (11),

$$\tilde{G}(\mathbf{z}) = e^{i\theta} \mathbf{z}^{-\mathbf{p}} \tilde{F}(\mathbf{z}) \quad \text{or} \quad e^{i\theta} \mathbf{z}^{-\mathbf{p}} \overline{\tilde{F}(1/\bar{\mathbf{z}})}, \quad \text{for some } \mathbf{p}, \theta \text{ and all } \mathbf{z}$$

which after substituting  $\mathbf{z} = \exp(-i2\pi\mathbf{w})$  becomes

$$\tilde{G}(e^{-i2\pi\mathbf{w}}) = e^{i\theta} e^{i\mathbf{w}\cdot\mathbf{p}} \tilde{F}(e^{-i2\pi\mathbf{w}}) \quad \text{or} \quad e^{i\theta} e^{i\mathbf{w}\cdot\mathbf{p}} \overline{\tilde{F}(e^{-i2\pi\mathbf{w}})}, \quad \text{for some } \mathbf{p}, \theta \text{ and all } \mathbf{z}.$$

Note that  $\tilde{G}(e^{-i2\pi\mathbf{w}})$  and  $\tilde{F}(e^{-i2\pi\mathbf{w}})$  are the Fourier transforms of  $\tilde{g}^0$  and  $\tilde{f}^0$ , respectively. Therefore in view of Remark 2.2 we have

$$\tilde{g}^0(\mathbf{n}) = e^{i\theta} \tilde{f}^0(\mathbf{n} - \mathbf{p}) \quad \text{or} \quad e^{i\theta} \text{Twin}(\tilde{f}^0)(\mathbf{n} - \mathbf{p}), \quad \forall \mathbf{n} \in \mathcal{M}^0,$$

which is equivalent to (12). □

### 3. Local uniqueness

First let us consider two-part ptychography where  $\mathcal{M} = \mathcal{M}^0 \cup \mathcal{M}^t$ .

We need two pieces of prior information: one on the mask phase and the anchoring assumption on an object part.

#### 3.1. Mask phase constraint (MPC)

Let  $\mu^0$  be a nonvanishing random mask with phase at each pixel distributed continuously and independently according to a probability density function  $p_\gamma$  nonvanishing in  $(-\gamma\pi, \gamma\pi]$  with a constant  $\gamma \leq 1$ .

Let

$$\alpha(\mathbf{n}) \exp[i\phi(\mathbf{n})] = \nu^0(\mathbf{n})/\mu^0(\mathbf{n}), \quad \alpha(\mathbf{n}) > 0, \quad \forall \mathbf{n} \in \mathcal{M}^0. \quad (13)$$

We say that  $\nu^0$  satisfies MPC( $\gamma$ ) if, for all  $\mathbf{n} \in \mathcal{M}^0$  and some constant  $\phi_0$

$$|\phi(\mathbf{n}) - \phi_0| \leq \delta\pi \pmod{2\pi}, \quad (14)$$

where

$$\delta < \min(\gamma, 1/2). \quad (15)$$

The larger  $\gamma$  is, the more phase diversity there is in the mask; the larger  $\delta$  is, the weaker the MPC( $\gamma$ ) is as a constraint. When  $\gamma > 1/2$ , MPC( $\gamma$ ) can be written simply as

$$\Re(\bar{\nu}^0(\mathbf{n})\mu^0(\mathbf{n})) > 0, \quad \forall \mathbf{n} \in \mathcal{M}^0. \quad (16)$$

We demonstrate the necessity of MPC( $\gamma$ ) in example 4.1.

The following theorem gives sufficient conditions of the local uniqueness for 2-part ptychography.

**Theorem 3.1.** Let  $f^0$  and  $f^t$  be a non-linear objects. Suppose that an arbitrary object  $g = g^0 \vee g^t$ , where  $g^0$  and  $g^t$  are defined on  $\mathcal{M}^0$  and  $\mathcal{M}^t$ , respectively, and an arbitrary mask  $\nu^0$  defined on  $\mathcal{M}^0$  produce the same ptychographic data as  $f$  and  $\mu^0$ . Moreover, suppose that  $\nu^0$  satisfies MPC( $\gamma$ ) and that  $f^0$  and  $g^0$  are an anchor, i.e.

$$\text{Box}[\text{supp}(\mathbf{f}^0)] = \text{Box}[\text{supp}(\mathbf{g}^0)] = \mathcal{M}^0. \quad (17)$$

Let

$$s = \min\{|\mathcal{S}_0|, |\mathcal{S}'_0|\} \geq 2 \quad (18)$$

where

$$\mathcal{S}_0 = \mathcal{M}^0 \cap \mathcal{M}^t \cap \text{supp}(f^0), \quad \mathcal{S}'_0 = \mathcal{M}^0 \cap \mathcal{M}^t \cap \text{supp}(\text{Twin}(\mathbf{f}^0)).$$

Then for some constants  $\theta_0, \theta_t \in \mathbb{R}$ , the following relations

$$\nu^0 \odot g^0 = e^{i\theta_0} \mu^0 \odot f^0 \quad (19)$$

$$\nu^t \odot g^t = e^{i\theta_t} \mu^t \odot f^t \quad (20)$$

hold true with probability at least

$$1 - c^s, \quad c < 1, \quad (21)$$

where the positive constant  $c$  depends only on  $\delta, \gamma, p_\gamma$  in MPC( $\gamma$ ).

**Remark 3.2.** The anchoring assumption can be relaxed to that of object support constraint (OSC) (see appendix A).

The proof of theorem 3.1 is given in appendix B.

Theorem 3.1 can be readily extended to the case of multi-part ptychography as follows.

Let  $\mathcal{T} = \{\mathbf{t}_k \in \mathbb{Z}^2 : k = 0, \dots, Q-1\}$  denote the set of all shifts in a ptychographic measurement. Let  $\mathcal{M}^k \equiv \mathcal{M}^{\mathbf{t}_k}$  and  $f^k \equiv f^{\mathbf{t}_k}$ .

We say that  $f^k$  and  $f^l$  are  $s$ -connected if

$$|\mathcal{M}^k \cap \mathcal{M}^l \cap \text{supp}(f)| \geq s \geq 2 \quad (22)$$

(see (18)) and that  $\{f^k : k = 1, \dots, Q-1\}$  are  $s$ -connected if there is an  $s$ -connected chain between any two elements.

**Theorem 3.3.** Let  $\{f^k, k = 0, \dots, Q-1\}$  be  $s$ -connected and every  $f^k$  is a non-linear part.

Suppose that an arbitrary object  $g = \bigvee_k g^k$ , where  $g^k$  are defined on  $\mathcal{M}^k$ , and a mask  $\nu^0$  defined on  $\mathcal{M}^0$  produce the same ptychographic data as  $f$  and  $\mu^0$ . Suppose that  $\nu^0$  satisfies MPC( $\gamma$ ) and hence

$$p := \max_{a \in \mathbb{R}} \Pr\{\Theta \in (a - 2\delta\pi, a + 2\delta\pi)\} < 1 \quad (23)$$

with  $\Theta$  distributed according to the probability density function  $p_\gamma \star p_\gamma$ .

In addition, suppose that for some  $\ell_0 \in \{0, 1, \dots, Q-1\}$   $f^{\ell_0}$  and  $g^{\ell_0}$  are an anchor or more generally

$$\nu^{\ell_0} \odot g^{\ell_0} = e^{i\theta_{\ell_0}} \mu^{\ell_0} \odot f^{\ell_0}. \quad (24)$$

Then with probability at least  $1 - 2Qp^s$ , we have

$$\nu^k \odot g^k = e^{i\theta_k} \mu^k \odot f^k, \quad k = 0, \dots, Q - 1, \quad (25)$$

for some constants  $\theta_k \in \mathbb{R}$ .

The proof of theorem 3.3 is given in appendix C.

#### 4. Ambiguities without MPC( $\gamma$ ) or anchoring assumption

The first example shows that (19) and (20) may fail in the absence of MPC( $\gamma$ ).

**Example 4.1.** Let  $\mathcal{M} = \mathbb{Z}_m \times \mathbb{Z}_n$ . Let  $m = 2n/3$  and  $\mathbf{t} = (m/2, 0)$ . Evenly partition  $f^0$  and  $f^{\mathbf{t}}$  into two parts as  $f^0 = [f_0^0, f_1^0]$  and  $f^{\mathbf{t}} = [f_0^1, f_1^1]$  with the overlap  $f_1^0 = f_0^1$  where  $f_j^i \in \mathbb{C}^{m \times m/2}$ ,  $i, j = 0, 1$ . Likewise, partition the mask as  $\mu^0 = [\mu_0^0, \mu_1^0]$ ,  $\mu^{\mathbf{t}} = [\mu_0^1, \mu_1^1]$  where  $\mu^{\mathbf{t}}$  is just the  $\mathbf{t}$ -shift of  $\mu^0$ , i.e.  $\mu^{\mathbf{t}}(\mathbf{n} + \mathbf{t}) = \mu^0(\mathbf{n})$ .

Suppose  $f_0^0 = f_1^1$  and consider the mask estimate  $\nu^0 = \text{Twin}(\mu^0)$  and the following object estimate: let

$$\begin{aligned} g^0 &= \text{Twin}(f^0) = [g_0^0, g_1^0] \\ g^{\mathbf{t}} &= \text{Twin}(f^{\mathbf{t}}) = [g_0^1, g_1^1] \end{aligned}$$

where  $g_1^0 = g_0^1$  due to  $f_0^0 = f_1^1$ , i.e.  $g = g^0 \vee g^{\mathbf{t}}$  is a well-defined object. The mask estimate  $\nu^0$  violates MPC( $\gamma$ ) because

$$\frac{\text{Twin}(\mu^0)(\mathbf{n})}{\mu^0(\mathbf{n})} = \frac{\bar{\mu}^0(\mathbf{N} - \mathbf{n})}{\mu^0(\mathbf{n})}, \quad \mathbf{n} \in \mathcal{M}^0,$$

has the maximum phase range  $(-2\gamma\pi, 2\gamma\pi]$ .

Clearly we have

$$\begin{aligned} \nu^0 \odot g^0 &= \text{Twin}(\mu^0 \odot f^0) \\ \nu^{\mathbf{t}} \odot g^{\mathbf{t}} &= \text{Twin}(\mu^{\mathbf{t}} \odot f^{\mathbf{t}}) \end{aligned}$$

so  $\nu^0$  and  $g$  produce the same ptychographic data as do  $\mu^0$  and  $f$  but violate (19) and (20) since in general

$$\begin{aligned} e^{i\theta_0} \mu^0 \odot f^0 &\neq \text{Twin}(\mu^0 \odot f^0) \\ e^{i\theta_{\mathbf{t}}} \mu^{\mathbf{t}} \odot f^{\mathbf{t}} &\neq \text{Twin}(\mu^{\mathbf{t}} \odot f^{\mathbf{t}}) \end{aligned}$$

for any  $\theta_0, \theta_{\mathbf{t}} \in \mathbb{R}$ .

The next example illustrates the translational and twin-like ambiguities associated with a loose object support (non-anchor).

**Example 4.2.** Assume the same set-up as in example 4.1 with the additional prior  $f_0^0 = f_1^1 = 0$ .

Let  $\nu^0 = \mu^0, \nu^t = \mu^t$  and  $g^0 = [g_0^0, 0], g^t = [0, g_1^t]$  where

$$\begin{aligned} g_0^0 &= f_1^0 \odot \mu_1^0 / \mu_0^0, \\ g_1^t &= f_0^1 \odot \mu_0^1 / \mu_1^1. \end{aligned}$$

Clearly,  $g = [g_0^0, 0, g_1^t]$  is different from  $f = [0, f_1^0, 0]$ .

It is straightforward to check that for  $\mathbf{m} = (m/2, 0)$

$$\begin{aligned} g^0(\mathbf{n})\nu^0(\mathbf{n}) &= f^0(\mathbf{n} + \mathbf{m})\mu^0(\mathbf{n} + \mathbf{m}), \quad \mathbf{n} \in \mathcal{M}^0 \\ g^t(\mathbf{n})\nu^t(\mathbf{n}) &= f^t(\mathbf{n} - \mathbf{m})\mu^t(\mathbf{n} - \mathbf{m}), \quad \mathbf{n} \in \mathcal{M}^t \end{aligned}$$

and hence  $g^0 \odot \mu^0$  and  $g^t \odot \mu^t$  produce the same diffraction patterns as  $f^0 \odot \mu^0$  and  $f^t \odot \mu^t$  for any  $\nu^0$ . In particular, by setting  $\nu^0 = \mu^0$ , we satisfy MPC with  $\delta = 0$ .

On the other hand, for  $\mathbf{m} \neq 0$  and any  $\theta_0, \theta_t \in \mathbb{R}$ ,

$$\begin{aligned} e^{i\theta_0} f^0 \odot \mu^0 &\neq f^0(\cdot + \mathbf{m}) \odot \mu^0(\cdot + \mathbf{m}) \\ e^{i\theta_t} f^t \odot \mu^t &\neq f^t(\cdot - \mathbf{m}) \odot \mu^t(\cdot - \mathbf{m}) \end{aligned}$$

in general and hence (19) and (20) are violated.

For the twin-like ambiguity, consider the same set-up with

$$g^0(\mathbf{n}) = \bar{f}^0(\mathbf{N} - \mathbf{n})\bar{\mu}^0(\mathbf{N} - \mathbf{n})/\mu^0(\mathbf{n}), \quad \forall \mathbf{n} \in \mathcal{M}^0 \quad (26)$$

$$g^t(\mathbf{n}) = \bar{f}^t(\mathbf{N} + 2\mathbf{t} - \mathbf{n})\bar{\mu}^t(\mathbf{N} + 2\mathbf{t} - \mathbf{n})/\mu^t(\mathbf{n}), \quad \forall \mathbf{n} \in \mathcal{M}^t. \quad (27)$$

Clearly,  $g = [g_0^0, 0, g_1^t]$  is different from  $f = [0, f_1^0, 0]$  but because

$$\begin{aligned} g^0(\mathbf{n})\nu^0(\mathbf{n}) &= \bar{f}^0(\mathbf{N} - \mathbf{n})\bar{\mu}^0(\mathbf{N} - \mathbf{n}), \quad \mathbf{n} \in \mathcal{M}^0 \\ g^t(\mathbf{n})\nu^t(\mathbf{n}) &= \bar{f}^t(\mathbf{N} + 2\mathbf{t} - \mathbf{n})\bar{\mu}^t(\mathbf{N} + 2\mathbf{t} - \mathbf{n}), \quad \mathbf{n} \in \mathcal{M}^t, \end{aligned}$$

$g^0 \odot \mu^0$  and  $g^t \odot \mu^t$ , as twin images, produce the same diffraction patterns as  $f^0 \odot \mu^0$  and  $f^t \odot \mu^t$  for any  $\nu^0$ . In particular, by setting  $\nu^0 = \mu^0$ , we satisfy MPC with  $\delta = 0$ .

On the other hand, (19) and (20) fail to hold since for any  $\theta_0, \theta_t \in \mathbb{R}$ ,

$$\begin{aligned} e^{i\theta_0} f^0 \odot \mu^0 &\neq \bar{f}^0(\mathbf{N} - \cdot) \odot \bar{\mu}^0(\mathbf{N} - \cdot) \\ e^{i\theta_t} f^t \odot \mu^t &\neq \bar{f}^t(\mathbf{N} + 2\mathbf{t} - \cdot) \odot \bar{\mu}^t(\mathbf{N} + 2\mathbf{t} - \cdot) \end{aligned}$$

in general.

## 5. Phase drift equation

In view of theorem 3.3, we make simple observations and transform (25) into the ambiguity equation that will be a key to subsequent development.

**Lemma 5.1.** *Let*

$$\alpha(\mathbf{n}) \exp[i\phi(\mathbf{n})] = \nu^0(\mathbf{n})/\mu^0(\mathbf{n}), \quad \alpha(\mathbf{n}) > 0, \quad \forall \mathbf{n} \in \mathcal{M}^0$$

and

$$h(\mathbf{n}) \equiv \ln g(\mathbf{n}) - \ln f(\mathbf{n}), \quad \forall \mathbf{n} \in \mathcal{M},$$

where  $f$  and  $g$  are assumed to be non-vanishing. Suppose that

$$\nu^k \odot g^k = e^{i\theta_k} \mu^k \odot f^k, \quad \forall k, \quad (28)$$

where  $\theta_k$  are constants. Then

$$h(\mathbf{n} + \mathbf{t}_k) = i\theta_k - \ln \alpha(\mathbf{n}) - i\phi(\mathbf{n}) \bmod i2\pi, \quad \forall \mathbf{n} \in \mathcal{M}^0, \quad (29)$$

and for all  $\mathbf{n} \in \mathcal{M}^k \cap \mathcal{M}^l$

$$\alpha(\mathbf{n} - \mathbf{t}_l) = \alpha(\mathbf{n} - \mathbf{t}_k) \quad (30)$$

$$\theta_k - \phi(\mathbf{n} - \mathbf{t}_k) = \theta_l - \phi(\mathbf{n} - \mathbf{t}_l) \bmod 2\pi. \quad (31)$$

**Remark 5.2.** The ambiguity equation (29) is a manifestation of local uniqueness (25) and has the immediate consequence

$$h(\mathbf{n} + \mathbf{t}_k) - h(\mathbf{n} + \mathbf{t}_l) = i\theta_k - i\theta_l \bmod i2\pi, \quad \forall \mathbf{n} \in \mathcal{M}^0, \quad \forall k, l \quad (32)$$

or equivalently

$$h(\mathbf{n} + \mathbf{t}_k - \mathbf{t}_l) - h(\mathbf{n}) = i\theta_k - i\theta_l \bmod i2\pi, \quad \forall \mathbf{n} \in \mathcal{M}^l \quad (33)$$

by shifting the argument in  $h$ .

We refer to (32) or (33) as the *phase drift equation* which determines the ambiguity (represented by  $h$ ) at different locations connected by Ptychographic shifts.

**Proof.** The ambiguity equation (29) follows immediately from (28) by taking logarithm on both sides.

By (28), for all  $\mathbf{n} \in \mathcal{M}^k \cap \mathcal{M}^l$ ,

$$g(\mathbf{n}) = e^{i\theta_k} f^k(\mathbf{n}) \mu^0(\mathbf{n} - \mathbf{t}_k) / \nu^0(\mathbf{n} - \mathbf{t}_k) = e^{i\theta_l} f^l(\mathbf{n}) \mu^0(\mathbf{n} - \mathbf{t}_l) / \nu^0(\mathbf{n} - \mathbf{t}_l). \quad (34)$$

We obtain by taking logarithm on both sides of (34) that

$$i\theta_l - i\theta_k - \ln f^k(\mathbf{n}) + \ln f^l(\mathbf{n}) + \ln \alpha(\mathbf{n} - \mathbf{t}_k) - \ln \alpha(\mathbf{n} - \mathbf{t}_l) + i\phi(\mathbf{n} - \mathbf{t}_k) - i\phi(\mathbf{n} - \mathbf{t}_l) = 0$$

modulo  $i2\pi$ . This implies that for  $\mathbf{n} \in \mathcal{M}^k \cap \mathcal{M}^l$

$$i\theta_l - i\theta_k + \ln \alpha(\mathbf{n} - \mathbf{t}_k) - \ln \alpha(\mathbf{n} - \mathbf{t}_l) + i\phi(\mathbf{n} - \mathbf{t}_k) - i\phi(\mathbf{n} - \mathbf{t}_l) = 0 \bmod i2\pi$$

which is equivalent to (30) and (31).  $\square$

## 6. Raster scan

To fix the idea, we set  $\mathcal{M} = \mathbb{Z}_n^2$  for the rest of the paper.

Note that no other assumptions than the anchoring assumption and the connectivity conditions, (18) and (22), are imposed on the scan scheme in theorem 3.3. In particular, theorem 3.3 applies to the regular raster scan which is more conveniently described in terms of two indices: for some  $q \in \mathbb{N}$ ,

$$\mathbf{t}_{kl} = \tau(k, l) = k\tau\mathbf{e}_1 + l\tau\mathbf{e}_2, \quad k, l = 0, \dots, q-1, \quad (35)$$

where  $\mathbf{e}_1 = (1, 0)$ ,  $\mathbf{e}_2 = (0, 1)$  and  $\tau$  is the constant step size of the raster scan. For simplicity of the set-up, we also assume that  $\tau = m/p = n/q$  for some integers  $p, q$  so that  $\mathbf{t}_{ql} = \mathbf{t}_{0l}$ ,  $\mathbf{t}_{kq} = \mathbf{t}_{0l}$  and the periodic boundary condition on  $\mathbb{Z}_n^2$  is satisfied.

We first show that the regular raster scan gives rise to an affine profile of block phase.

**Proposition 6.1.** *Under the assumptions of Lemma 5.1, the block phase  $\{\theta_{kl}\}$  for the raster scan (35) has an affine profile:*

$$\theta_{kl} = \theta_{00} + r_1k + r_2l \quad (36)$$

for  $r_1, r_2 \in \mathbb{R}$ .

**Remark 6.2.** Due to the affine phase ambiguity,  $r_1$  and  $r_2$  are undetermined constants.

**Proof.** By (32), for all  $\mathbf{n} \in \mathcal{M}^{00} \cap (\mathcal{M}^{00} - (\tau, 0))$ ,

$$h(\mathbf{n} + (\tau, 0)) = h(\mathbf{n}) + i\theta_{10} - i\theta_{00} \quad (37)$$

and hence

$$\begin{aligned} h(\mathbf{n} + \mathbf{t}_{kl}) &= h(\mathbf{n}) + i\theta_{kl} - i\theta_{00} \\ &= h(\mathbf{n} + (\tau, 0)) + i\theta_{kl} - i\theta_{10}. \end{aligned} \quad (38)$$

On the other hand, (32) also implies

$$h(\mathbf{n} + (\tau, 0) + \mathbf{t}_{kl}) = h(\mathbf{n} + (\tau, 0)) + i\theta_{kl} - i\theta_{00} \quad (39)$$

and by (38)

$$\begin{aligned} h(\mathbf{n} + (\tau, 0) + \mathbf{t}_{kl}) &= h(\mathbf{n} + \mathbf{t}_{kl}) - i\theta_{kl} + i\theta_{10} + i\theta_{kl} - i\theta_{00} \\ &= h(\mathbf{n} + \mathbf{t}_{kl}) + i\theta_{10} - i\theta_{00} \end{aligned} \quad (40)$$

for all  $\mathbf{n} \in \mathcal{M}^{00} \cap (\mathcal{M}^{00} - (\tau, 0))$ .

By induction with (40), we have

$$h(\mathbf{n} + (\tau, 0) + \mathbf{t}_{kl}) = h(\mathbf{n} + \mathbf{t}_{0l}) + (k+1)i(\theta_{10} - \theta_{00}). \quad (41)$$

Likewise, we also have

$$h(\mathbf{n} + (0, \tau) + \mathbf{t}_{kl}) = h(\mathbf{n} + \mathbf{t}_{k0}) + (l+1)i(\theta_{01} - \theta_{00}). \quad (42)$$

Combining (41) and (42) with (32), we arrive at the desired result (36) with

$$r_1 = \theta_{10} - \theta_{00}, \quad r_2 = \theta_{01} - \theta_{00}. \quad \square$$

**Corollary 6.3.** For the raster scan (35) with  $\tau = 1$ , we have

$$h(\mathbf{n}) = h(0) + \mathbf{i}\mathbf{n} \cdot (r_1, r_2) \bmod i2\pi, \tag{43}$$

$$\phi(\mathbf{n}) = \theta_{00} - \Im[h(0)] - \mathbf{n} \cdot (r_1, r_2) \bmod 2\pi \tag{44}$$

$$\alpha = e^{-\Re[h(0)]} \tag{45}$$

$$\theta_{kl} = \theta_{00} + kr_1 + lr_2, \quad k, l = 0, \dots, n - 1, \tag{46}$$

for all  $\mathbf{n} \in \mathbb{Z}_n^2$  and some  $r_1, r_2 \in \mathbb{R}$ .

**Proof.** Setting  $\tau = 1$  in (41) and (42), we have the identity (43).

By (29),

$$h(\mathbf{n} + \mathbf{t}) = i\theta_{\mathbf{t}} - \ln \alpha(\mathbf{n}) - i\phi(\mathbf{n}) \bmod i2\pi, \quad \forall \mathbf{t} \in \mathcal{T}. \tag{47}$$

With  $\mathbf{t} = \mathbf{t}_{00}$ , (47) and (43) imply (44) and (45).

The relation (46) follows from (47) and

$$h(\mathbf{n} + \mathbf{t}) = h(0) + \mathbf{i}(\mathbf{n} + \mathbf{t}) \cdot (r_1, r_2)$$

for any  $\mathbf{t} \in \mathcal{T}$ . Note that the argument for (46) is an independent proof from proposition 6.1. □

The expressions (43) and (44) correspond to the affine phase ambiguity while (45) is the scaling factor ambiguity.

Even though the global uniqueness (43) and (46) is our goal but the raster scan with  $\tau = 1$  has too much redundancy and is impractical. On the other hand, when  $\tau > 1$ , there are many additional ambiguities associated with the regular raster scan, posing substantial challenge to blind ptychographic reconstruction [13]. Two of these ambiguities are illustrated below.

The first example shows the ambiguity induced by the affine profile of the block phase (36).

**Example 6.4.** For  $q = 3, \tau = m/2$ , let

$$f = \begin{bmatrix} f_{00} & f_{10} & f_{20} \\ f_{01} & f_{11} & f_{21} \\ f_{02} & f_{12} & f_{22} \end{bmatrix}$$

$$g = \begin{bmatrix} f_{00} & e^{i2\pi/3}f_{10} & e^{i4\pi/3}f_{20} \\ e^{i2\pi/3}f_{01} & e^{i4\pi/3}f_{11} & f_{21} \\ e^{i4\pi/3}f_{02} & f_{12} & e^{i2\pi/3}f_{22} \end{bmatrix}$$

be the object and its reconstruction, respectively, where  $f_{ij} \in \mathbb{C}^{n/3 \times n/3}$ . Let

$$\mu^{kl} = \begin{bmatrix} \mu_{00}^{kl} & \mu_{10}^{kl} \\ \mu_{01}^{kl} & \mu_{11}^{kl} \end{bmatrix}, \quad \nu^{kl} = \begin{bmatrix} \mu_{00}^{kl} & e^{-i2\pi/3} \mu_{10}^{kl} \\ e^{-i2\pi/3} \mu_{01}^{kl} & e^{-i4\pi/3} \mu_{11}^{kl} \end{bmatrix},$$

$k, l = 0, 1, 2$ , be the  $(k, l)$ th shift of the probe and estimate, respectively, where  $\mu_{ij}^{kl} \in \mathbb{C}^{n/3 \times n/3}$ .

Let  $f^{ij}$  and  $g^{ij}$  be the part of the object and estimate masked by  $\mu^{ij}$  and  $\nu^{ij}$ , respectively. For example, we have

$$f^{00} = \begin{bmatrix} f_{00} & f_{10} \\ f_{01} & f_{11} \end{bmatrix}, \quad f^{10} = \begin{bmatrix} f_{10} & f_{20} \\ f_{11} & f_{21} \end{bmatrix}, \quad f^{20} = \begin{bmatrix} f_{20} & f_{00} \\ f_{21} & f_{01} \end{bmatrix}$$

and likewise for other  $f^{ij}$  and  $g^{ij}$ . It is easily seen that  $\nu^{ij} \odot g^{ij} = e^{i(i+j)2\pi/3} \mu^{ij} \odot f^{ij}$ .

The next example illustrates the periodic artifact called the raster grid pathology.

**Example 6.5.** For  $q = 3, \tau = m/2$  and any  $\psi \in \mathbb{C}^{\frac{n}{3} \times \frac{n}{3}}$ , let

$$f = \begin{bmatrix} f_{00} & f_{10} & f_{20} \\ f_{01} & f_{11} & f_{21} \\ f_{02} & f_{12} & f_{22} \end{bmatrix}$$

$$g = \begin{bmatrix} e^{-i\psi} \odot f_{00} & e^{-i\psi} \odot f_{10} & e^{-i\psi} \odot f_{20} \\ e^{-i\psi} \odot f_{01} & e^{-i\psi} \odot f_{11} & e^{-i\psi} \odot f_{21} \\ e^{-i\psi} \odot f_{02} & e^{-i\psi} \odot f_{12} & e^{-i\psi} \odot f_{22} \end{bmatrix}$$

be the object and its reconstruction, respectively, where  $f_{ij} \in \mathbb{C}^{n/3 \times n/3}$ . Let

$$\mu^{kl} = \begin{bmatrix} \mu_{00}^{kl} & \mu_{10}^{kl} \\ \mu_{01}^{kl} & \mu_{11}^{kl} \end{bmatrix}, \quad \nu^{kl} = \begin{bmatrix} e^{i\psi} \odot \mu_{00}^{kl} & e^{i\psi} \odot \mu_{10}^{kl} \\ e^{i\psi} \odot \mu_{01}^{kl} & e^{i\psi} \odot \mu_{11}^{kl} \end{bmatrix},$$

$k, l = 0, 1, 2$ , be the  $(k, l)$ th shift of the probe and estimate, respectively, where  $\mu_{ij}^{kl} \in \mathbb{C}^{n/3 \times n/3}$ .

Let  $f^{ij}$  and  $g^{ij}$  be the part of the object and estimate illuminated by  $\mu^{ij}$  and  $\nu^{ij}$ , respectively (as in example 6.4). It is verified easily that  $\nu^{ij} \odot g^{ij} = \mu^{ij} \odot f^{ij}$ .

The overlap ratio of above examples is 50% (since  $\tau = m/2$ ). However, the above construction of ambiguities can be easily extended to the raster scan with any overlap ratio. Moreover, all other ambiguities for blind ptychography with the raster scan can be shown to be the combinations of the above two types of ambiguity [13].

On the other hand, in the case  $\tau = 1$  ( $q = n$ ), the ambiguity in example 6.4 is identical to the affine phase ambiguity (1) and (2) while the ambiguity in example 6.5 becomes the constant phase factor inherent to any phase retrieval.

For the rest of the paper, we develop an approach to characterizing a more general class of scan schemes that enjoy the global uniqueness property (43)–(46) by leveraging the phase drift equations (32) and (33) more effectively. We refer to such schemes as *ptychographically complete* schemes.

## 7. Motivating example: perturbed raster scan

Consider small perturbations to the raster scan:

$$\mathbf{t}_{kl} = \tau(k, l) + (\delta_{kl}^1, \delta_{kl}^2), \quad k, l = 0, \dots, q-1 \quad (48)$$

where  $\tau = n/q$ ,  $\mathbf{t}_{ql} = \mathbf{t}_{0l}$ ,  $\mathbf{t}_{kq} = \mathbf{t}_{0l}$  (the periodic boundary condition) and  $\delta_{kl}^1, \delta_{kl}^2$  are small integers. Without loss of generality, we set  $\delta_{00}^1 = \delta_{00}^2 = 0$  and hence  $\mathbf{t}_{00} = (0, 0)$ , see figure 6(b).

We assume the *non-overstepping* condition that the perturbations do not change the ordering of  $\{\mathbf{t}_{kl}\}$ , i.e.

$$\tau + \delta_{k+1,l}^1 - \delta_{kl}^1 > 0, \quad \tau + \delta_{k,l+1}^2 - \delta_{kl}^2 > 0, \quad k, l = 0, \dots, q-1. \quad (49)$$



**Figure 5.** Shortest paths (in the Manhattan distance) from the lower-right corner  $(1, -1)$  to the upper-left corner  $(0, 0)$  in the diagrams spanned by  $\mathbf{t}_{kl} - \mathbf{t}_{k-1,l}$  and  $\mathbf{t}_{k+1,l} - \mathbf{t}_{kl}$ . The left diagram corresponds to  $\sigma_1$  in (52) and the right diagram to  $\sigma_2$  in (53).

Consider the triplet  $(\mathbf{t}_{k-1,l}, \mathbf{t}_{kl}, \mathbf{t}_{k+1,l})$  for any  $k, l$  and let

$$\mathbf{a}_{kl}^1 := (\mathbf{t}_{kl} - \mathbf{t}_{k-1,l}) - (\mathbf{t}_{k+1,l} - \mathbf{t}_{kl}) = 2\delta_{kl}^1 - \delta_{k-1,l}^1 - \delta_{k+1,l}^1, \tag{50}$$

implying

$$h(\mathbf{n} + 2\mathbf{t}_{kl} - \mathbf{t}_{k+1,l} - \mathbf{t}_{k-1,l}) = h(\mathbf{n} + \mathbf{a}_{kl}^1). \tag{51}$$

We want to reduce the lefthand side of (51) to  $h(\mathbf{n})$  by using (33) repeatedly.

There are at least two paths for reduction:

$$\sigma_1 : (\mathbf{t}_{kl} - \mathbf{t}_{k-1,l}) - (\mathbf{t}_{k+1,l} - \mathbf{t}_{kl}) \longrightarrow \mathbf{t}_{kl} - \mathbf{t}_{k-1,l} \longrightarrow 0 \tag{52}$$

$$\sigma_2 : (\mathbf{t}_{kl} - \mathbf{t}_{k-1,l}) - (\mathbf{t}_{k+1,l} - \mathbf{t}_{kl}) \longrightarrow -(\mathbf{t}_{k+1,l} - \mathbf{t}_{kl}) \longrightarrow 0, \tag{53}$$

corresponding to the two paths depicted in figure 5. Following  $\sigma_1$ , we have the identities

$$\begin{aligned} h(\mathbf{n} + \mathbf{a}_{kl}^1) &= h(\mathbf{n} + \mathbf{t}_{kl} - \mathbf{t}_{k-1,l}) + i\theta_{kl} - i\theta_{k+1,l}, \quad \forall \mathbf{n} \in \mathcal{M}^{kl} - \mathbf{a}_{kl}^1 \\ &= h(\mathbf{n}) + i(2\theta_{kl} - \theta_{k-1,l} - \theta_{k+1,l}) \quad \forall \mathbf{n} \in \mathcal{M}^{kl} - \mathbf{t}_{kl} + \mathbf{t}_{k-1,l} \end{aligned}$$

implying

$$h(\mathbf{n} + \mathbf{a}_{kl}^1) = h(\mathbf{n}) + i(2\theta_{kl} - \theta_{k-1,l} - \theta_{k+1,l}) \tag{54}$$

for all  $\mathbf{n}$  in the set

$$[\mathcal{M}^{kl} - \mathbf{a}_{kl}^1] \cap [\mathcal{M}^{kl} - \mathbf{t}_{kl} + \mathbf{t}_{k-1,l}]. \tag{55}$$

On the other hand, following  $\sigma_2$  we have the identities

$$\begin{aligned} h(\mathbf{n} + \mathbf{a}_{kl}^1) &= h(\mathbf{n} + \mathbf{t}_{10} - \mathbf{t}_{00}) + i\theta_{10} - i\theta_{20}, \quad \forall \mathbf{n} \in \mathcal{M}^{kl} - \mathbf{a}_{kl}^1 \\ &= h(\mathbf{n}) + i(2\theta_{kl} - \theta_{k-1,l} - \theta_{k+1,l}) \quad \forall \mathbf{n} \in \mathcal{M}^{kl} - \mathbf{t}_{kl} + \mathbf{t}_{k+1,l} \end{aligned}$$

implying (54) for all  $\mathbf{n}$  in the set

$$[\mathcal{M}^{kl} - \mathbf{a}_{kl}^1] \cap [\mathcal{M}^{kl} - \mathbf{t}_{kl} + \mathbf{t}_{k+1,l}]. \tag{56}$$

Combining the two routes of reduction, we have

$$h(\mathbf{n} + \mathbf{a}_{kl}^1) = h(\mathbf{n}) + i(2\theta_{kl} - \theta_{k+1,l} - \theta_{k-1,l}) \tag{57}$$

(modulo  $i2\pi$ ) for all  $\mathbf{n}$  in the set  $(\mathcal{M}^{kl} - \mathbf{a}_{kl}^1) \cap D_{kl}^1$  where

$$\begin{aligned} D_{kl}^1 &:= (\mathcal{M}^{kl} - \mathbf{t}_{kl} + \mathbf{t}_{k-1,l}) \cup (\mathcal{M}^{kl} - \mathbf{t}_{kl} + \mathbf{t}_{k+1,l}) \\ &= \mathcal{M}^{k-1,l} \cup \mathcal{M}^{k+1,l}. \end{aligned} \tag{58}$$

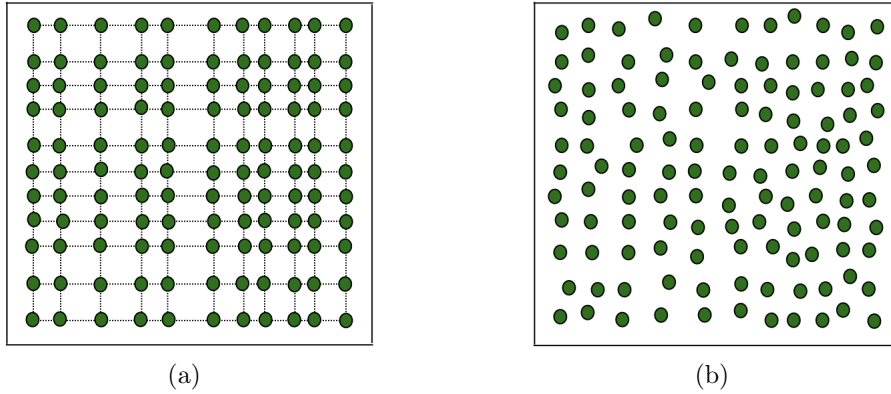


**Figure 6.** Two perturbed raster scans. (a) Perturbed grid given by (64). (b) Perturbed grid given by (48).

Likewise, with

$$\mathbf{a}_{kl}^2 := (\mathbf{t}_{kl} - \mathbf{t}_{k,l-1}) - (\mathbf{t}_{k,l+1} - \mathbf{t}_{kl}) = 2\delta_{kl}^2 - \delta_{k,l-1}^2 - \delta_{k,l+1}^2 \tag{59}$$

we have

$$h(\mathbf{n} + \mathbf{a}_{kl}^2) = h(\mathbf{n}) + i(2\theta_{kl} - \theta_{k,l+1} - \theta_{k,l-1}) \tag{60}$$

(modulo  $i2\pi$ ) for all  $\mathbf{n}$  in the set  $D_{k,l}^2 \cap (\mathcal{M}^{k,l-1} - \mathbf{a}_{kl}^2)$  where

$$\begin{aligned} D_{k,l}^2 &:= (\mathcal{M}^{kl} - \mathbf{t}_{kl} + \mathbf{t}_{k,l-1}) \cup (\mathcal{M}^{kl} - \mathbf{t}_{kl} + \mathbf{t}_{k,l+1}) \\ &= \mathcal{M}^{k,l-1} \cup \mathcal{M}^{k,l+1}. \end{aligned} \tag{61}$$

Repeatedly using (33), we can prove that the relation (57) and (60) hold respectively in the sets

$$\bigcup_{\mathbf{t} \in \mathcal{T}} [\mathbf{t} - \mathbf{t}_{kl} + (\mathcal{M}^{k-1,l} \cup \mathcal{M}^{k+1,l}) \cap (\mathcal{M}^{kl} - \mathbf{a}_{kl}^1) \cap \mathcal{M}^{kl}] \tag{62}$$

and

$$\bigcup_{\mathbf{t} \in \mathcal{T}} [\mathbf{t} - \mathbf{t}_{kl} + (\mathcal{M}^{k,l-1} \cup \mathcal{M}^{k,l+1}) \cap (\mathcal{M}^{kl} - \mathbf{a}_{kl}^2) \cap \mathcal{M}^{kl}] \tag{63}$$

where the additional restriction due to the presence of  $\mathcal{M}^{kl}$  is to ensure the validity of applying (33) (See lemma 8.2 for a proof in a more general setting).

For a special class of perturbed raster scans, precise conditions for the sets in (62) and (63) to cover  $\mathbb{Z}_n^2$  can be simply stated as follows.

**Lemma 7.1.** For the perturbed raster scan (48) with the non-overstepping condition (49), suppose

$$\delta_{kl}^1 = \delta_k^1, \quad \delta_{kl}^2 = \delta_l^2, \quad \forall k, l = 0, \dots, q-1. \tag{64}$$

(Consequently,  $\mathbf{a}_{kl}^1 = \mathbf{a}_k^1, \mathbf{a}_{kl}^2 = \mathbf{a}_l^2$ ) see figure 6(b).

If for some fixed  $k, l$ ,

$$2\tau \leq m + \max\{\delta_{k-1}^1 - \delta_{k+1}^1, \delta_{l-1}^2 - \delta_{l+1}^2\} \tag{65}$$

and

$$\max_{i=1,2} [|a_k^i| + \max_{k'} \{\delta_{k'+1}^i - \delta_{k'}^i\}] \leq m - \tau, \tag{66}$$

where

$$a_k^1 = 2\delta_k^1 - \delta_{k-1}^1 - \delta_{k+1}^1, \quad a_l^2 = 2\delta_l^2 - \delta_{l-1}^2 - \delta_{l+1}^2,$$

then each set in (62) and (63) contains  $\mathbb{Z}_n^2$ .

**Remark 7.2.** For the raster scan (35),  $a_k^1 = a_l^2 = 0$  for all  $k, l$ .

For small perturbations  $\delta_k^1, \delta_l^2 \ll 1$ , (66) is satisfied and (65) means an overlap ratio slightly greater than 50%. This is an improved and simplified version of the one given in [13].

**Proof.** First (65) implies that the right edge of  $\mathcal{M}^{k-1,l}$  is no less than the left edge of  $\mathcal{M}^{k+1,l}$  by more than one pixel and that the upper edge of  $\mathcal{M}^{k-1,l}$  is no less than the lower edge of  $\mathcal{M}^{k,l+1}$  by more than one pixel. Hence both  $\mathcal{M}^{k-1,l} \cup \mathcal{M}^{k+1,l}$  and  $\mathcal{M}^{k,l-1} \cup \mathcal{M}^{k,l+1}$  are rectangles and by the non-overstepping condition (49)

$$\mathcal{M}^{k-1,l} \cup \mathcal{M}^{k+1,l} \supseteq \mathcal{M}^{kl}, \quad \mathcal{M}^{k,l-1} \cup \mathcal{M}^{k,l+1} \supseteq \mathcal{M}^{kl}.$$

For the remaining argument, it suffices to show that

$$\mathbb{Z}_n^2 \subseteq \bigcup_{\mathbf{t} \in \mathcal{T}} [\mathbf{t} - \mathbf{t}_{kl} + (\mathcal{M}^{kl} - \mathbf{a}_k^1) \cap \mathcal{M}^{kl}], \quad \mathbb{Z}_n^2 \subseteq \bigcup_{\mathbf{t} \in \mathcal{T}} [\mathbf{t} - \mathbf{t}_{kl} + (\mathcal{M}^{kl} - \mathbf{a}_l^2) \cap \mathcal{M}^{kl}]. \tag{67}$$

To this end, since the intersection of two adjacent sets in (67)

$$\{\mathbf{t}_{ij} - \mathbf{t}_{kl} + \mathcal{M}^{kl} \cap (\mathcal{M}^{kl} - \mathbf{a}_k^1)\} \cap \{\mathbf{t}_{i+1,j} - \mathbf{t}_{kl} + \mathcal{M}^{kl} \cap (\mathcal{M}^{kl} - \mathbf{a}_k^1)\} \tag{68}$$

$$\{\mathbf{t}_{ij} - \mathbf{t}_{kl} + \mathcal{M}^{kl} \cap (\mathcal{M}^{kl} - \mathbf{a}_l^2)\} \cap \{\mathbf{t}_{i,j+1} - \mathbf{t}_{kl} + \mathcal{M}^{kl} \cap (\mathcal{M}^{kl} - \mathbf{a}_l^2)\} \tag{69}$$

are congruent to

$$\{\mathcal{M}^{00} \cap (\mathcal{M}^{00} - (a_k^1, 0))\} \cap \{(\tau + \delta_{i+1}^1 - \delta_i^1, 0) + \mathcal{M}^{00} \cap (\mathcal{M}^{00} - (a_k^1, 0))\} \\ \{\mathcal{M}^{00} \cap (\mathcal{M}^{00} - (0, a_l^2))\} \cap \{(0, \tau + \delta_{j+1}^2 - \delta_j^2) + \mathcal{M}^{00} \cap (\mathcal{M}^{00} - (0, a_l^2))\},$$

(66) implies that neither set in (68) and (69) is empty for any  $i, j$ . Therefore (67) holds true.  $\square$

The following is an immediate consequence of (57), (60) and lemma 7.1.

**Corollary 7.3.** Suppose that  $f$  does not vanish in  $\mathbb{Z}_n^2$ . Under the assumptions of lemma 7.1, if

$$a_k^1 = 1, \quad a_l^2 = 1, \quad \text{for some } k, l, \tag{70}$$

then the scheme isptychographically complete, i.e.

$$h(\mathbf{n}) = h(0) + \mathbf{n} \cdot (r_1, r_2) \bmod i2\pi \tag{71}$$

$$\phi(\mathbf{n}) = \theta_{00} - \Im[h(0)] - \mathbf{n} \cdot (r_1, r_2) \bmod 2\pi \tag{72}$$

$$\alpha = e^{-\Re[h(0)]} \quad (73)$$

$$\theta_{\mathbf{t}} = \theta_{00} + \mathbf{t} \cdot (r_1, r_2) \bmod 2\pi, \quad \mathbf{t} \in \mathcal{T}, \quad (74)$$

for all  $\mathbf{n} \in \mathbb{Z}_n^2$  where  $r_1, r_2 \in \mathbb{R}$  are undetermined constants (due to the affine phase ambiguity).

**Proof.** The assumption (70), (57), (60) and lemma 7.1 imply that

$$h(\mathbf{n} + \mathbf{e}_1) = h(\mathbf{n}) + i(2\theta_{kl} - \theta_{k+1,l} - \theta_{k-1,l}), \quad h(\mathbf{n} + \mathbf{e}_2) = h(\mathbf{n}) + i(2\theta_{kl} - \theta_{k,l+1} - \theta_{k,l-1})$$

for all  $\mathbf{n}$  in  $\mathbb{Z}_n^2$  and hence (71).

The rest of the proof is exactly the same as that of corollary 6.3. In particular, (74) follows from (71) and the phase drift equations (32) and (33).  $\square$

More generally, we have the following global uniqueness theorem for the perturbed raster scan (64).

**Theorem 7.4.** *Suppose that  $f$  does not vanish in  $\mathbb{Z}_n^2$ . For the perturbed raster scan (64) satisfying the non-overstepping condition (49) let  $\{(\delta_{k_i}^1, \delta_{l_j}^2) : i, j\}$  be any nonempty subset of perturbations satisfying (65) and (66) in lemma 7.1.*

Let

$$a_i^1 = 2\delta_{k_i}^1 - \delta_{k_{i-1}}^1 - \delta_{k_{i+1}}^1, \quad a_j^2 = 2\delta_{l_j}^2 - \delta_{l_{j-1}}^2 - \delta_{l_{j+1}}^2, \quad \forall i, j,$$

and suppose

$$\gcd(|a_i^1|) = \gcd(|a_j^2|) = 1 \quad (75)$$

where  $\gcd$  denotes the greatest common divisor. Then the global uniqueness (71)–(74) holds true and the scheme is ptychographically complete.

**Proof.** The coprime condition (75) implies the existence of  $c_i^1, c_j^2 \in \mathbb{Z}$  such that

$$\sum_i c_i^1 a_i^1 = \sum_j c_j^2 a_j^2 = 1. \quad (76)$$

By repeatedly using (57) and (60) we have

$$h(\mathbf{n} + \mathbf{e}_1) = h\left(\mathbf{n} + \left(\sum_i c_i^1 a_i^1, 0\right)\right) = h(\mathbf{n}) + ir_1 \bmod i2\pi$$

$$h(\mathbf{n} + \mathbf{e}_2) = h\left(\mathbf{n} + \left(0, \sum_j c_j^2 a_j^2\right)\right) = h(\mathbf{n}) + ir_2 \bmod i2\pi$$

where

$$r_1 = \sum_i c_i^1 (2\theta_{k_i, i} - \theta_{k_{i+1}, i} - \theta_{k_{i-1}, i}), \quad r_2 = \sum_j c_j^2 (2\theta_{i, l_j} - \theta_{i, l_{j+1}} - \theta_{i, l_{j-1}})$$

and hence (71).  $\square$

Instead of linear shifts with uneven step sizes in (64), the general case (48) produces curvilinear shifts which is more difficult to analyze. To state the analogous theorem for the general case (48), let  $\mathbf{u}_i := (u_{i1}, u_{i2}), i = 1, 2$ , be a  $\mathbb{Z}^2$ -lattice basis, i.e. the four integers  $u_{11}, u_{12}, u_{21}, u_{22}$  satisfy

$$u_{11}u_{22} - u_{12}u_{21} = 1. \quad (77)$$

Since  $u_{11}u_{22} - u_{12}u_{21} = 1$ , there exist integers  $b_{ij}, i, j = 1, 2$ , such that

$$b_{11}\mathbf{u}_1 + b_{12}\mathbf{u}_2 = \mathbf{e}_1 = (1, 0), \quad b_{21}\mathbf{u}_1 + b_{22}\mathbf{u}_2 = \mathbf{e}_2 = (0, 1).$$

**Theorem 7.5.** *Suppose that  $f$  does not vanish in  $\mathbb{Z}_n^2$ . For the perturbed raster scan (48) satisfying the non-overstepping condition (49), let  $\{(\delta_{k_i l_i}^1, \delta_{k_j l_j}^2) : i, j\}$  be any nonempty subset of perturbations such that*

$$\mathbb{Z}_n^2 \subseteq \bigcup_{\mathbf{t} \in \mathcal{T}} [\mathbf{t} - \mathbf{t}_{k_i l_i} + (\mathcal{M}^{k_i-1, l_i} \cup \mathcal{M}^{k_i+1, l_i}) \cap (\mathcal{M}^{k_i l_i} - \mathbf{a}_{k_i}^1) \cap \mathcal{M}^{k_i l_i}], \quad \forall i \quad (78)$$

and

$$\mathbb{Z}_n^2 \subseteq \bigcup_{\mathbf{t} \in \mathcal{T}} [\mathbf{t} - \mathbf{t}_{k_j l_j} + (\mathcal{M}^{k_j l_j-1} \cup \mathcal{M}^{k_j l_j+1}) \cap (\mathcal{M}^{k_j l_j} - \mathbf{a}_{l_j}^2) \cap \mathcal{M}^{k_j l_j}], \quad \forall j. \quad (79)$$

Let

$$\mathbf{a}_i^1 := (\mathbf{t}_{k_i l_i} - \mathbf{t}_{k_i-1, l_i}) - (\mathbf{t}_{k_i+1, l_i} - \mathbf{t}_{k_i l_i}), \quad \forall i \quad (80)$$

$$\mathbf{a}_j^2 := (\mathbf{t}_{k_j l_j} - \mathbf{t}_{k_j, l_j-1}) - (\mathbf{t}_{k_j, l_j+1} - \mathbf{t}_{k_j l_j}), \quad \forall j \quad (81)$$

and suppose that

$$\sum_i c_i^1 \mathbf{a}_i^1 = \mathbf{u}_1, \quad \sum_j c_j^2 \mathbf{a}_j^2 = \mathbf{u}_2 \quad (82)$$

for some  $c_i^1, c_j^2 \in \mathbb{Z}$  where  $\{\mathbf{u}_1, \mathbf{u}_2\}$  is a  $\mathbb{Z}^2$ -lattice basis. Then the global uniqueness (71)–(74) holds true and the scheme is ptychographically complete.

**Remark 7.6.** The conditions (78) and (79) are tedious to state in terms of the perturbations  $\delta_{kl}^1, \delta_{kl}^2$  and do not provide much insight beyond what is given in remark 7.2.

**Proof.** As before, we begin with

$$h(\mathbf{n} + \mathbf{a}_i^1) = h(\mathbf{n}) + i(2\mathbf{t}_{k_i l_i} - \mathbf{t}_{k_i-1, l_i} - \mathbf{t}_{k_i+1, l_i})$$

$$h(\mathbf{n} + \mathbf{a}_j^2) = h(\mathbf{n}) + i(2\mathbf{t}_{k_j l_j} - \mathbf{t}_{k_j, l_j-1} - \mathbf{t}_{k_j, l_j+1})$$

(mod  $i2\pi$ ) for all  $\mathbf{n} \in \mathbb{Z}_n^2$  and repeatedly use (82) to obtain

$$h(\mathbf{n} + \mathbf{u}_1) = h(\mathbf{n}) + i\Delta_1, \quad h(\mathbf{n} + \mathbf{u}_2) = h(\mathbf{n}) + i\Delta_2$$

where

$$\begin{aligned}\Delta_1 &= \sum_i c_i^1 (2\theta_{k_i l_i} - \theta_{k_i+1, l_i} - \theta_{k_i-1, l_i}) \\ \Delta_2 &= \sum_j c_j^2 (2\theta_{k_j l_j} - \theta_{k_j, l_j+1} - \theta_{k_j, l_j-1}).\end{aligned}$$

Since  $u_{11}u_{22} - u_{12}u_{21} = 1$ , there exist integers  $b_{ij}, i, j = 1, 2$ , such that

$$b_{11}\mathbf{u}_1 + b_{12}\mathbf{u}_2 = \mathbf{e}_1, \quad b_{21}\mathbf{u}_1 + b_{22}\mathbf{u}_2 = \mathbf{e}_2.$$

Therefore, for  $j = 1, 2$ ,

$$\begin{aligned}h(\mathbf{n} + \mathbf{e}_1) &= h(\mathbf{n}) + ib_{11}\Delta_1 + ib_{12}\Delta_2 \\ h(\mathbf{n} + \mathbf{e}_2) &= h(\mathbf{n}) + ib_{21}\Delta_1 + ib_{22}\Delta_2,\end{aligned}$$

and (71)–(74) hold true. □

## 8. Mixing schemes with three-part coupling

Let us begin with a simple example showing that a perturbed scan with overlap ratios less than 50% may result in excessive ambiguities.

**Example 8.1.** Let us consider the perturbed scheme (64) with  $q = 2$  and

$$\mathbf{t}_{kl} = (\tau_k, \tau_l), \quad k, l = 0, 1, 2 \tag{83}$$

where  $\tau_0 = 0, \tau_2 = n$  and

$$3m/2 < n < m + \tau_1. \tag{84}$$

The condition (84) is to ensure that the overlap ratio  $(2 - n/m)$  between two adjacent blocks is less than (but can be made arbitrarily close to) 50%. To avoid the raster scan (which has many undesirable ambiguities [13]), we assume that  $\tau_1 \neq n/2$  and hence  $\tau_2 \neq 2\tau_1$ . Note that the periodic boundary condition implies that  $\mathcal{M}^{00} = \mathcal{M}^{20} = \mathcal{M}^{02} = \mathcal{M}^{22}$ . Figure 7 illustrates the relative positions of  $\mathcal{M}^{00}$  and  $\mathcal{M}^{10}$ .

First let us focus on the horizontal shifts  $\{\mathbf{t}_{k0} : k = 0, 1, 2\}$ . As shown in figure 7, two subsets of  $\mathcal{M} = \mathbb{Z}_n^2$

$$R_{00} = \llbracket m + \tau_1 - n, \tau_1 - 1 \rrbracket \times \mathbb{Z}_m, \quad R_{10} = \llbracket m, n - 1 \rrbracket \times \mathbb{Z}_m$$

are covered only once by  $\mathcal{M}^{00}$  and  $\mathcal{M}^{10}$  respectively due to the (84). It is straightforward to check that the conclusion of lemma 7.1 fails in this case.

Now consider the intersections

$$\begin{aligned}\tilde{R}_{10} &:= R_{10} \cap (\mathbf{t}_{10} + R_{00}) = R_{10} \cap \llbracket m + 2\tau_1 - n, 2\tau_1 - 1 \rrbracket \times \mathbb{Z}_m \\ \tilde{R}_{00} &:= (R_{10} - \mathbf{t}_{10}) \cap R_{00} = \llbracket m - \tau_1, n - \tau_1 - 1 \rrbracket \times \mathbb{Z}_m \cap R_{00}\end{aligned}$$

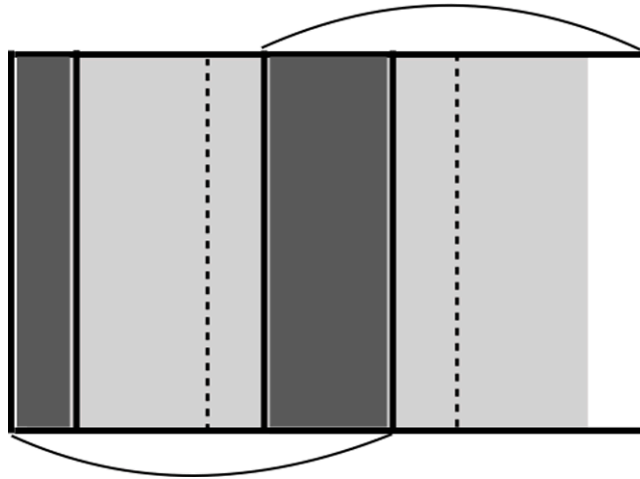


**Figure 7.** A perturbed scan with  $q = 2$ . The arcs indicate the extend of the two blocks  $\mathcal{M}^{00}$  and  $\mathcal{M}^{10}$ . The dotted lines mark the midlines of the two blocks. The grey area represents the object with the light grey areas being  $R_{00}$  and  $R_{10}$  and the dark grey areas being the overlap of the two blocks. The white area inside  $\mathcal{M}^{10}$  folds into the other end inside  $\mathcal{M}^{00}$  by the periodic boundary condition.

which respectively correspond to the same region of the mask in  $\mathcal{M}^{10}$  and  $\mathcal{M}^{00}$  and let  $h_1$  be any function defined on  $\mathcal{M}$  such that  $h_1(\mathbf{n}) = 0$  for any  $\mathbf{n} \notin \tilde{R}_{10} \cup \tilde{R}_{00}$  and  $h_1(\mathbf{n} + \mathbf{t}_1) = h_1(\mathbf{n})$  for any  $\mathbf{n} \in \tilde{R}_{00}$ .

Consider the object estimate  $g(\mathbf{n}) = e^{h_1(\mathbf{n})}f(\mathbf{n})$  and the mask estimate  $\nu^{k0}(\mathbf{n}) := e^{-h_1(\mathbf{n})}\mu^{k0}(\mathbf{n})$ , which is well defined because  $\tilde{R}_{10} = \mathbf{t}_{10} + \tilde{R}_{00}$  and both correspond to the same region of the mask.

By the same token, we can construct a similar ambiguity function  $h_2$  for the vertical shifts. With both horizontal and vertical shifts, we define the ambiguity function  $h = h_1h_2$  and the associated pair of mask-object estimate  $\nu^{kl}(\mathbf{n}) := e^{-h(\mathbf{n})}\mu^{kl}(\mathbf{n})$  and  $g(\mathbf{n}) = e^{h(\mathbf{n})}f(\mathbf{n})$ .

Clearly, the mask-object pair  $(\nu, g)$  produces the identical set of diffraction patterns as  $(\mu, f)$ . Therefore this ptychographic scheme has at least  $(2\tau_1 - m)^2$  or  $(2n - 2\tau_1 - m)^2$  degrees of ambiguity dimension depending on whether  $2\tau_1 < n$  or  $2\tau_1 > n$ .

The above construction of the ambiguity function  $h$  extends to a perturbed scan (64) with any  $q \geq 2$  and overlap ratios less than 50%. More importantly,  $\tilde{R}_{00}$  and  $\tilde{R}_{10}$  illustrate the notion of *singly covered invariant regions* which may be present in more general schemes of low overlap ratio.

A singly covered invariant region  $R$  is the union of congruent subsets  $R_j \subset \mathcal{M}^j$  each of which is covered *once only* by the same subset  $S \subset \mathcal{M}^0$  of the mask, i.e.  $R_j = \mathbf{t}_j + S$  for all  $j$ . As in example 8.1, the existence of such an invariant region entails an ambiguity function  $h$  that is any function defined on  $\mathcal{M}$  such that  $h(\mathbf{n}) = 0$  for any  $\mathbf{n} \notin R$  and  $h(\mathbf{n} + \mathbf{t}_j) = h(\mathbf{n})$  for all  $\mathbf{n}$ . In other words, every component region  $R_j$  is infected with the same ambiguity which is transported by the mask region  $S$  from component to component. The ambiguity dimension equals the size of each component region  $R_j$ .



**Proof.** For any fixed  $\sigma$ , we know from the above analysis that (91) holds true for all  $\mathbf{n}$  in the set (90).

By (33),

$$h(\mathbf{n} + \mathbf{t}_l - \mathbf{t}_k) = h(\mathbf{n}) + i\theta_l - i\theta_k, \quad \forall \mathbf{n} \in \mathcal{M}^k,$$

and by (89)

$$\begin{aligned} h(\mathbf{n} + \mathbf{a} + \mathbf{t}_l - \mathbf{t}_k) &= h(\mathbf{n} + \mathbf{a}) + i\theta_l - i\theta_k \\ &= h(\mathbf{n}) - ip_2(\theta_{k+1} - \theta_k) + ip_1(\theta_k - \theta_{k-1}) + i\theta_l - i\theta_k. \end{aligned}$$

Hence we have

$$h(\mathbf{n} + \mathbf{a} + \mathbf{t}_l - \mathbf{t}_k) = h(\mathbf{n} + \mathbf{t}_l - \mathbf{t}_k) - ip_2(\theta_{k+1} - \theta_k) + ip_1(\theta_k - \theta_{k-1}).$$

In other words, (91) is valid in the set  $\mathbf{t}_l - \mathbf{t}_k + \mathcal{M}^k \cap (\mathcal{M}^k - \mathbf{a}) \cap D_k(\sigma, \mathbf{s}_1, \mathbf{s}_2)$ . Taking the union over all shifts and paths, we obtain (92).  $\square$

We now define the *mixing* schemes that connect different parts of the object by the ptychographic shifts in a non-degenerate manner.

### 8.1. The mixing property

Let  $\{(j_i^s, k_i^s, l_i^s)\}, s = 1, 2$ , be a non-empty subset of triplets of index such that for some  $p_i^s, q_i^s \in \mathbb{Z}$

$$\mathbb{Z}_n^2 \subseteq \bigcup_{\mathbf{t} \in \mathcal{T}} \bigcup_{\sigma} \left[ \mathbf{t} - \mathbf{t}_{k_i^s} + D_i(\sigma, \mathbf{t}_{k_i^s} - \mathbf{t}_{j_i^s}, \mathbf{t}_{l_i^s} - \mathbf{t}_{k_i^s}) \cap (\mathcal{M}^{k_i^s} - \mathbf{a}_i^s) \cap \mathcal{M}^{k_i^s} \right] \quad (93)$$

where  $\sigma \in \Pi(p_i^s, -q_i^s, \mathbf{t}_{k_i^s} - \mathbf{t}_{j_i^s}, \mathbf{t}_{l_i^s} - \mathbf{t}_{k_i^s})$  and  $\mathbf{a}_i^s := p_i^s(\mathbf{t}_{k_i^s} - \mathbf{t}_{j_i^s}) - q_i^s(\mathbf{t}_{l_i^s} - \mathbf{t}_{k_i^s})$ .

Moreover, for some  $c_i^s \in \mathbb{Z}$

$$\sum_i c_i^1 \mathbf{a}_i^1 = \mathbf{u}_1, \quad \sum_i c_i^2 \mathbf{a}_i^2 = \mathbf{u}_2 \quad (94)$$

where  $\{\mathbf{u}_1, \mathbf{u}_2\}$  is a  $\mathbb{Z}^2$ -lattice basis.

As seen in theorems 7.4 and 7.5, the most tedious part of the above definition is (93) when the set  $D_i(\sigma, \mathbf{t}_{k_i^s} - \mathbf{t}_{j_i^s}, \mathbf{t}_{l_i^s} - \mathbf{t}_{k_i^s}) \cap (\mathcal{M}^{k_i^s} - \mathbf{a}_i^s) \cap \mathcal{M}^{k_i^s}$  is not rectangular.

The mixing schemes are so named because the propagation of ambiguity by the ptychographic shifts, according to the phase drift equations (32) and (33), is so complete that a distinct ambiguity profile (affine phase + scaling factor) emerges as a result.

We can state the global uniqueness theorem for the mixing schemes whose proof is entirely analogous to that of theorem 7.5.

**Theorem 8.3.** *Suppose  $\text{supp}(f) = \mathbb{Z}_n^2$ . If  $\mathcal{T}$  satisfies the mixing property, then*

$$h(\mathbf{n}) = h(0) + \mathbf{n} \cdot (r_1, r_2) \bmod i2\pi, \quad (95)$$

$$\phi(\mathbf{n}) = \theta_0 - \Im[h(0)] - \mathbf{n} \cdot (r_1, r_2) \bmod 2\pi \quad (96)$$

$$\alpha = e^{-\Re[h(0)]} \quad (97)$$

$$\theta_{\mathbf{t}} = \theta_0 + \mathbf{t} \cdot (r_1, r_2) \bmod 2\pi, \quad \forall \mathbf{t} \in \mathcal{T}, \quad (98)$$

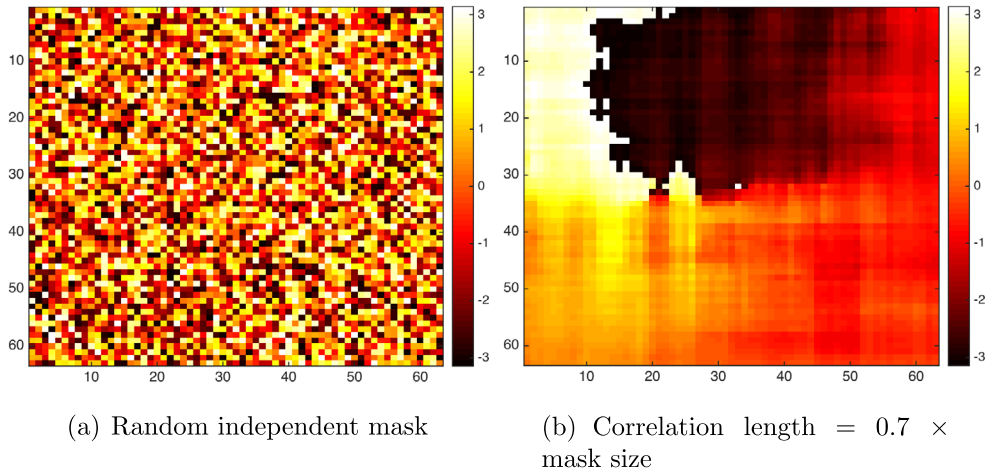


**Figure 9.** The phase profile of (a) the random independent mask and (b) the correlated mask of correlation length equal to 0.7 mask size.

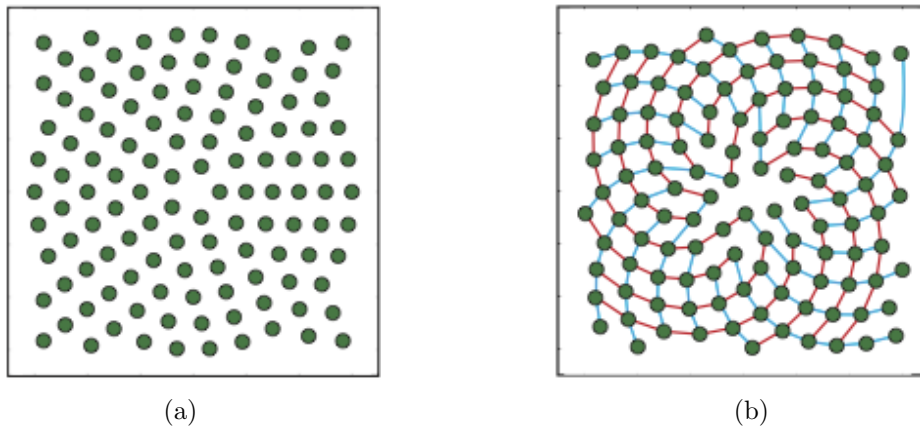


**Figure 10.** Special scans that have good empirical performances [9, 21, 24]. (a) Concentric circles. (b) Fermat spiral.

for some  $r_1, r_2 \in \mathbb{R}$  and all  $\mathbf{n} \in \mathbb{Z}_n^2$ .

## 9. Conclusion and discussion

Under the MPC and the anchoring assumption, we have proved, for a strongly connected object, the local uniqueness (theorem 3.1 and theorem 3.3) manifested as the phase drift equations (32) and (33). We have shown by examples (examples 4.1 and 4.2) that both MPC and the anchoring assumption are necessary. For the global uniqueness with the exception of inherent ambiguities (scaling factor and affine phase factor), we have showed that the mixing schemes are ptychographically complete (theorem 8.3), including the perturbed raster scans (theorems 7.4 and 7.5).

In addition, for both the mixing schemes and the regular raster scan (proposition 6.1), we have proved that their block phases must have an affine profile,  $\theta_{\mathbf{t}} = \theta_0 + \mathbf{t} \cdot \mathbf{r}$  for some  $\mathbf{r} \in \mathbb{R}^2$ . It is unclear if this holds true for any other schemes without the global uniqueness property.

Our approach to global uniqueness is based on 3-part coupling designed particularly for analyzing the perturbed raster scans. Our theory and example 8.1 prove that the overlap ratio 50% is more or less the minimum requirement for blind ptychography with the irregularly perturbed raster scan (see (75) and (82)).

Our theory has several practical implications. First, the connectivity condition (4) suggests that in the case of a sparse object a higher overlap ratio may be required. Second, MPC is re-interpretable in terms of other measurement uncertainties such as scan position errors [20]. The level of scan position off-sets that can be corrected depends on the type of mask used in measurement. For a random independent mask (figure 9(a)), MPC corresponds to correctable position error of about half a pixel; For a correlated mask, MPC corresponds to correctable position error on the order of the correlation length.

In other words, there is a trade-off between the mask correlation length and the correctable level of scan position error. Numerical evidence suggests that with the same MPC a highly correlated mask (figure 9(b)) performs only slightly worse than the random independent mask [17]. As mechanical and thermal vibrations are inevitable, it makes sense to use a mask of a comparable correlation length to compensate for scan position offset. On the other hand, a simple regular mask (e.g. Fresnel illumination spot) is often a sub-optimal choice as twin-like ambiguities may be present even with perfect knowledge of the mask [7]. In addition, a random mask has the benefit of producing more diffuse illumination and thus data of lower dynamic-range.

Another implication of MPC is in numerical reconstruction. MPC is independent of the knowledge about the mask amplitude, meaning that the knowledge about the mask phase is much more important for blind ptychography. Indeed, MPC turns out to be an effective method for mask initialization, yielding geometrically convergent iterations, even when the initialization error (measured in L2 norm) is large [17].

One is naturally led to the important question of optimal scan schemes which use the minimum number of diffraction patterns for a given object (i.e. the minimum redundancy in measurement) to be ptychographically complete. The measurement redundancy is more or less proportional to the product of the number of adjacent blocks and the overlap ratio. Our results show that the irregularly perturbed raster scans with overlap ratio slightly over 50% is optimal among the class of perturbed raster scans. For more general scans, the minimum overlap requirement may be lowered and 5-part or higher order coupling must be directly accounted for. For example, the Fermat spiral scan scheme (figure 10(b)) is claimed to provide a more uniform coverage than the perturbed raster scans and the concentric circle pattern (figure 10(a)), thus lowering the overlap ratio [24]. A rigorous theory for general optimal scans, however, is beyond the scope of the present work and has to be left for future research.

## Acknowledgments

The research of AF is supported by the US National Science Foundation Grant DMS-1413373. The present work was initiated during a stimulating and fruitful visit of AF to National Center for Theoretical Sciences (NCTS), Taiwan, in October 2017. Research of PC is supported in part

by the Grant MOST 107-2115-M-005-006-MY3 from Ministry of Science and Technology, Taiwan.

## Appendix A. Object support constraint (OSC)

Instead of a tight support, an object part may possess various degrees of loose support depending on the scan position and size of the block (see figure 3). The looseness of support can be characterized by a set of admissible shifts  $T_0$  as follows.

**Object support constraint (OSC).** An object estimate  $g^0$  satisfies the OSC with respect to a given set of shifts  $T_0$  if  $\mathbf{m} \in T_0$  whenever

$$\text{supp}(g^0) \quad \text{or} \quad \text{supp}(\text{Twin}(g^0)) \subseteq \text{Box}[\text{supp}(\mathbf{f}^0)] - \mathbf{m}. \quad (\text{A.1})$$

We can use OSC to describe the precision of our prior knowledge about  $\text{Box}[\text{supp}(\mathbf{f}^0)]$  when  $f^0$  has a loose support in  $\mathcal{M}^0$ . The smaller the set  $T_0$  is, the more precise the OSC is. When  $\text{Box}[\text{supp}(\mathbf{f}^0)] = \mathcal{M}^0$ , we can set  $T_0 = \{(0,0)\}$  since the condition (A.1) becomes

$$\text{supp}(g^0) \quad \text{or} \quad \text{supp}(\text{Twin}(g^0)) \subseteq \mathcal{M}^0 \quad (\text{A.2})$$

which is null and gives no new information.

Under OSC, the quantity  $s$  in (18) is defined instead as

$$s = \min_{\mathbf{m}, \mathbf{m}' \in T_0} |S_0(\mathbf{m})| \wedge |S'_0(\mathbf{m}')| \geq 2 \quad (\text{A.3})$$

where  $T_0$  is the set of shifts in OSC and

$$\begin{aligned} S_0(\mathbf{m}) &= \mathcal{M}^0 \cap \mathcal{M}^t \cap (\text{supp}(f^0) - \mathbf{m}) \\ S'_0(\mathbf{m}) &= \mathcal{M}^0 \cap \mathcal{M}^t \cap (\text{supp}(\text{Twin}(f^0)) + \mathbf{m}). \end{aligned}$$

The construction in example 4.2 satisfies the OSC (A.1) with

$$T_0 = \{(a, 0) : a = 0, \dots, m/2\}.$$

On the other hand, if  $f_1^0, f_0^1$  are non-vanishing, then it can be verified that  $s = 0$ , consistent with the fact that the probability for ambiguity is one as shown in the above construction.

However, if we enhance the precision of the support knowledge by tightening  $T_0$  by any amount  $l \geq 1$  as

$$T_0 = \{(a, 0) : a = 0, \dots, m/2 - l\}, \quad (\text{A.4})$$

then the constructions would violate the OSC (A.1), and be rejected. Moreover, for (A.4),  $s = ml$  with nonvanishing  $f_1^0, f_0^1$  so the probability of uniqueness is closed to one for  $m \gg 1$  as predicted by theorem 3.1.

Although OSC is more general than the anchoring assumption, it is also more complicated and less practical so we do not pursue the full proof here. For the interested reader, we refer to the preliminary version [14] for the proof of theorem 3.1 under the assumption of OSC.

## Appendix B. Proof of theorem 3.1

Let  $\mathbf{N} = (m, m)$ . Applying corollary 2.4 to both  $\mathcal{M}^0$  and  $\mathcal{M}^t$  we have the following alternatives: for some  $\mathbf{m}_1, \mathbf{m}_2 \in \mathbb{Z}^2, \theta_0, \theta_t \in \mathbb{R}$ .

$$\begin{aligned}
g^0(\mathbf{n}) &= e^{i\theta_0} f^0(\mathbf{n} + \mathbf{m}_1) \mu^0(\mathbf{n} + \mathbf{m}_1) / \nu^0(\mathbf{n}) \\
\text{or } \text{Twin}(\mathbf{g}^0)(\mathbf{n}) &= e^{-i\theta_0} f^0(\mathbf{n} + \mathbf{m}_1) \mu^0(\mathbf{n} + \mathbf{m}_1) / \text{Twin}(\nu^0)(\mathbf{n}), \quad \forall \mathbf{n} \in \mathcal{M}^0
\end{aligned} \tag{B.1}$$

and

$$\begin{aligned}
g^{\mathbf{t}}(\mathbf{n}) &= e^{i\theta_{\mathbf{t}}} f^{\mathbf{t}}(\mathbf{n} + \mathbf{m}_2) \mu^{\mathbf{t}}(\mathbf{n} + \mathbf{m}_2) / \nu^{\mathbf{t}}(\mathbf{n}) \\
\text{or } \text{Twin}(\mathbf{g}^{\mathbf{t}})(\mathbf{n}) &= e^{-i\theta_{\mathbf{t}}} f^{\mathbf{t}}(\mathbf{n} + \mathbf{m}_2) \mu^{\mathbf{t}}(\mathbf{n} + \mathbf{m}_2) / \text{Twin}(\nu^{\mathbf{t}})(\mathbf{n}), \quad \forall \mathbf{n} \in \mathcal{M}^{\mathbf{t}}.
\end{aligned} \tag{B.2}$$

Note that  $\text{Twin}(\mathbf{g}^{\mathbf{t}})(\mathbf{n}) = \bar{g}^{\mathbf{t}}(\mathbf{N} + 2\mathbf{t} - \mathbf{n})$  so we can rewrite (B.1) and (B.2) as

$$\begin{aligned}
g^0(\mathbf{n}) &= e^{i\theta_0} f^0(\mathbf{n} + \mathbf{m}_1) \mu^0(\mathbf{n} + \mathbf{m}_1) / \nu^0(\mathbf{n}) \\
\text{or } e^{i\theta_0} \bar{f}^0(\mathbf{N} - \mathbf{n} + \mathbf{m}_1) \bar{\mu}^0(\mathbf{N} - \mathbf{n} + \mathbf{m}_1) / \nu^0(\mathbf{n}), \quad \forall \mathbf{n} \in \mathcal{M}^0
\end{aligned} \tag{B.3}$$

and

$$\begin{aligned}
g^{\mathbf{t}}(\mathbf{n}) &= e^{i\theta_{\mathbf{t}}} f^{\mathbf{t}}(\mathbf{n} + \mathbf{m}_2) \mu^0(\mathbf{n} + \mathbf{m}_2 - \mathbf{t}) / \nu^0(\mathbf{n} - \mathbf{t}) \\
\text{or } e^{i\theta_{\mathbf{t}}} \bar{f}^{\mathbf{t}}(\mathbf{N} + 2\mathbf{t} - \mathbf{n} + \mathbf{m}_2) \bar{\mu}^0(\mathbf{N} + \mathbf{t} - \mathbf{n} + \mathbf{m}_2) / \nu^0(\mathbf{n} - \mathbf{t}), \quad \forall \mathbf{n} \in \mathcal{M}^{\mathbf{t}}
\end{aligned} \tag{B.4}$$

for some  $\mathbf{m}_1, \mathbf{m}_2 \in \mathbb{Z}, \theta_0, \theta_{\mathbf{t}} \in \mathbb{R}$  where we have used the relation  $\mu^{\mathbf{t}}(\cdot) = \mu^0(\cdot - \mathbf{t}), \nu^{\mathbf{t}}(\cdot) = \nu^0(\cdot - \mathbf{t})$ . Note that  $\mathbf{N}$  and  $\mathbf{N} + \mathbf{t} = (m + t_1, m + t_2)$  are the upper-right corners of  $\mathcal{M}^0$  and  $\mathcal{M}^{\mathbf{t}}$ , respectively.

In view of the anchoring assumption, (B.1) implies  $\mathbf{m}_1 = 0$ .

We now focus on the intersection  $\mathcal{M}^0 \cap \mathcal{M}^{\mathbf{t}}$  where (B.3) and (B.4) both hold. We have then four possible ambiguities from the crossover of the alternatives in (B.3) and (B.4).

**Case (i).** The combination of the first alternatives in (B.3) and (B.4) imply that for all  $\mathbf{n} \in \mathcal{M}^0 \cap \mathcal{M}^{\mathbf{t}}$

$$e^{i\theta_0} f^0(\mathbf{n}) \mu^0(\mathbf{n}) / \nu^0(\mathbf{n}) = e^{i\theta_{\mathbf{t}}} f^{\mathbf{t}}(\mathbf{n} + \mathbf{m}_2) \mu^0(\mathbf{n} - \mathbf{t} + \mathbf{m}_2) / \nu^0(\mathbf{n} - \mathbf{t}) \tag{B.5}$$

provided that  $f^0(\mathbf{n})$  and  $f^{\mathbf{t}}(\mathbf{n} + \mathbf{m}_2)$  are both zero or nonzero.

We now show that with high probability (B.5) fails to hold for some  $\mathbf{n} \in \mathcal{M}^0 \cap \mathcal{M}^{\mathbf{t}}$ .

Consider any  $\mathbf{n} \in S_0$  (hence  $f^0(\mathbf{n}) \neq 0$ ) and assume that  $f^{\mathbf{t}}(\mathbf{n} + \mathbf{m}_2) \neq 0$ . Otherwise, (B.5) holds with probability zero.

We obtain by taking logarithm on both sides of (B.5) that

$$\begin{aligned}
&\ln \mu^0(\mathbf{n}) + \ln \mu^0(\mathbf{n} - \mathbf{t}) - \ln \mu^0(\mathbf{n} - \mathbf{t} + \mathbf{m}_2) - \ln \mu^0(\mathbf{n}) \\
&= i\theta_{\mathbf{t}} - i\theta_0 - \ln f^0(\mathbf{n}) + \ln f^{\mathbf{t}}(\mathbf{n} + \mathbf{m}_2) + \ln \alpha(\mathbf{n}) - \ln \alpha(\mathbf{n} - \mathbf{t}) \\
&\quad + i\phi(\mathbf{n}) - i\phi(\mathbf{n} - \mathbf{t})
\end{aligned} \tag{B.6}$$

modulo  $i2\pi$ . We want to show that if  $|S_0|$  is sufficiently large then (B.6) holds with at most exponentially small probability.

Since  $\mathbf{n} \in \mathcal{M}^0 \cap \mathcal{M}^{\mathbf{t}}$  and  $\mathbf{n} + \mathbf{m}_2 \in \mathcal{M}^{\mathbf{t}}$ , the points associated with the lefthand side of (B.6),  $\mathbf{n} - \mathbf{t}, \mathbf{n} + \mathbf{m}_2 - \mathbf{t}$ , belong in  $\mathcal{M}^0$ . Hence the random variables on the lefthand side of (B.6) are well-defined and have a finite value.

The two points  $\mathbf{n} - \mathbf{t}, \mathbf{n} + \mathbf{m}_2 - \mathbf{t}$  can not be identical unless  $\mathbf{m}_2 = 0$ . In other words, if  $\mathbf{m}_2 \neq 0$ , then the imaginary part  $\Theta_1$  of the lefthand side of (B.6)

$$\Theta_1 := \theta(\mathbf{n} - \mathbf{t}) - \theta(\mathbf{n} - \mathbf{t} + \mathbf{m}_2) \quad (\text{B.7})$$

is the sum of two independent random variables and hence the support set of its probability density contains  $(-2\gamma\pi, 2\gamma\pi]$ .

On the righthand side of (B.6), however, as  $f^0(\mathbf{n})$  and  $f^{\mathbf{t}}(\mathbf{n} + \mathbf{m}_2)$  are given (hence deterministic), the phase fluctuation is determined by  $\phi(\mathbf{n}) - \phi(\mathbf{n} - \mathbf{t})$  which ranges over the interval  $(-2\delta\pi, 2\delta\pi]$  due to the constraint (14). Consequently (B.6) holds true with probability at most

$$p_1 := \max_{a \in \mathbb{R}} \Pr\{\Theta_1 \in (a - 2\delta\pi, a + 2\delta\pi]\} < 1,$$

for each  $\mathbf{n}$ , since  $\delta < \min(\gamma, \frac{1}{2})$ .

For all  $\mathbf{n} \in S_0$ , there are at least  $|S_0|/2!$  statistically independent instances, corresponding to the number of *non-intersecting*  $\{\mathbf{n} - \mathbf{t}, \mathbf{n} + \mathbf{m}_2 - \mathbf{t}\}$ . Therefore (B.6) holds true with probability at most  $p_1^{|S_0|/2!}$  unless  $\mathbf{m}_2 = 0$ .

On the other hand, for  $\mathbf{m}_2 = 0$ , the desired result (19) and (20) follows directly from the first alternatives in (B.3) and (B.4).

**Case (ii).** Consider the combination of the first alternative in (B.3) and the second alternative in (B.4) that for  $\mathbf{n} \in \mathcal{M}^0 \cap \mathcal{M}^{\mathbf{t}}$

$$\begin{aligned} g(\mathbf{n}) &= e^{i\theta_0} f^0(\mathbf{n}) \mu^0(\mathbf{n}) / \nu^0(\mathbf{n}) \\ &= e^{i\theta_0} \bar{f}^{\mathbf{t}}(\mathbf{N} + 2\mathbf{t} - \mathbf{n} + \mathbf{m}_2) \bar{\mu}^0(\mathbf{N} + \mathbf{t} - \mathbf{n} + \mathbf{m}_2) / \nu^0(\mathbf{n} - \mathbf{t}), \end{aligned} \quad (\text{B.8})$$

provided that  $f^0(\mathbf{n})$  and  $\bar{f}^{\mathbf{t}}(\mathbf{N} + 2\mathbf{t} - \mathbf{n} + \mathbf{m}_2)$  are both zero or nonzero.

Consider any  $\mathbf{n} \in S_0$  (hence  $f^0(\mathbf{n}) \neq 0$ ) and assume  $\bar{f}^{\mathbf{t}}(\mathbf{N} + 2\mathbf{t} - \mathbf{n} + \mathbf{m}_2) \neq 0$ . Otherwise (B.8) is false and can be ruled out.

Taking logarithm and rearranging terms in (B.8) we have

$$\begin{aligned} &\ln \mu^0(\mathbf{n}) + \ln \mu^0(\mathbf{n} - \mathbf{t}) - \ln \bar{\mu}^0(\mathbf{N} + \mathbf{t} - \mathbf{n} + \mathbf{m}_2) - \ln \mu^0(\mathbf{n}) \\ &= i\theta_{\mathbf{t}} - i\theta_0 - \ln f^0(\mathbf{n}) + \ln \bar{f}^{\mathbf{t}}(\mathbf{N} + 2\mathbf{t} - \mathbf{n} + \mathbf{m}_2) + \ln \alpha(\mathbf{n}) - \ln \alpha(\mathbf{n} - \mathbf{t}) \\ &\quad + i\phi(\mathbf{n}) - i\phi(\mathbf{n} - \mathbf{t}). \end{aligned} \quad (\text{B.9})$$

The imaginary parts of the lefthand side of (B.9)

$$\Theta_2 := \theta(\mathbf{n} - \mathbf{t}) + \theta(\mathbf{N} + \mathbf{t} - \mathbf{n} + \mathbf{m}_2) \quad (\text{B.10})$$

is the sum of two independent random variables unless

$$\mathbf{n} = \mathbf{t} + \frac{1}{2}(\mathbf{N} + \mathbf{m}_2),$$

in which case  $\Theta_2 = 2\theta(\mathbf{n} - \mathbf{t})$ . Since  $|S_0| \geq 2$ , there exists some  $\mathbf{n} \in S_0$  such that  $\Theta_2$  is the sum of two independent random variables and hence the support of its probability density function contains  $(-2\gamma\pi, 2\gamma\pi]$ . By the same argument as above, (B.9) holds true with probability at most  $p_2^{|S_0(\mathbf{m}_2)|/2!}$  where

$$p_2 := \max_{a \in \mathbb{R}} \Pr\{\Theta_2 \in (a - 2\delta\pi, a + 2\delta\pi]\} < 1$$

since  $\delta < \min(\gamma, \frac{1}{2})$ .

**Case (iii).** Consider the combination of the second alternative in (B.3) and the first alternative in (B.4) that for  $\mathbf{n} \in \mathcal{M}^0 \cap \mathcal{M}^t$

$$\begin{aligned} g(\mathbf{n}) &= e^{i\theta_0 \bar{f}^0(\mathbf{N} - \mathbf{n})} \bar{\mu}^0(\mathbf{N} - \mathbf{n}) / \nu^0(\mathbf{n}) \\ &= e^{i\theta_t \bar{f}^t(\mathbf{n} + \mathbf{m}_2)} \mu^0(\mathbf{n} - \mathbf{t} + \mathbf{m}_2) / \nu^0(\mathbf{n} - \mathbf{t}) \end{aligned} \tag{B.11}$$

provided that  $f^0(\mathbf{n})$  and  $f^t(\mathbf{N} + 2\mathbf{t} - \mathbf{n} + \mathbf{m}_2)$  are both zero or nonzero. Consider any  $\mathbf{n} \in S'_0$  (hence  $\bar{f}^0(\mathbf{N} - \mathbf{n}) \neq 0$ ) and assume  $f^t(\mathbf{n} + \mathbf{m}_2) \neq 0$ . Otherwise (B.12) can be ruled out.

Taking logarithm and rearranging terms in (B.11) we have

$$\begin{aligned} &\ln \bar{\mu}^0(\mathbf{N} - \mathbf{n}) + \ln \mu^0(\mathbf{n} - \mathbf{t}) - \ln \mu^0(\mathbf{n} - \mathbf{t} + \mathbf{m}_2) - \ln \nu^0(\mathbf{n}) \\ &= i\theta_t - i\theta_0 - \ln \bar{f}^0(\mathbf{N} - \mathbf{n}) + \ln f^t(\mathbf{n} + \mathbf{m}_2) + \ln \alpha(\mathbf{n}) - \ln \alpha(\mathbf{n} - \mathbf{t}) \\ &+ i\phi(\mathbf{n}) - i\phi(\mathbf{n} - \mathbf{t}). \end{aligned} \tag{B.12}$$

As before, we want to show that if  $|S'_0|$  is sufficiently large, then (B.12) holds with at most exponentially small probability.

Since  $\mathbf{n} \in \mathcal{M}^0 \cap \mathcal{M}^t$  and  $\mathbf{n} + \mathbf{m}_2 \in \mathcal{M}^t$ , the four points associated with the lefthand side of (B.12),  $\mathbf{N} - \mathbf{n}, \mathbf{n} - \mathbf{t}, \mathbf{n} - \mathbf{t} + \mathbf{m}_2, \mathbf{n}$ , belong in  $\mathcal{M}^0$ . Hence the four random variables on the lefthand side of (B.12) are well-defined.

The imaginary parts of the lefthand side of (B.12) given by

$$\Theta_3 := -\theta(\mathbf{N} - \mathbf{n}) + \theta(\mathbf{n} - \mathbf{t}) - \theta(\mathbf{n} - \mathbf{t} + \mathbf{m}_2) - \theta(\mathbf{n}) \tag{B.13}$$

is the sum of two, three or four independent random variables unless

$$\mathbf{m}_2 = 0, \quad \mathbf{n} = \frac{1}{2}\mathbf{N}, \tag{B.14}$$

in which case  $\Theta_3 = 2\theta(\mathbf{N}/2)$ .

Since  $S'_0 \geq 2$ , there exists some  $\mathbf{n} \in S'_0$  such that  $\Theta_2$  is the sum of at least two independent random variables and hence the support of its probability density function contains  $(-2\gamma\pi, 2\gamma\pi]$ .

On the righthand side of (B.12), the phase fluctuation is determined by  $\phi(\mathbf{n}) - \phi(\mathbf{n} - \mathbf{t})$  which ranges over the interval  $(-2\delta\pi, 2\delta\pi]$  due to the MPC( $\gamma$ ) (14). So (B.12) holds true with probability at most

$$p_3 := \max_{a \in \mathbb{R}} \Pr\{\Theta_3 \in (a - 2\delta\pi, a + 2\delta\pi]\} < 1$$

for each  $\mathbf{n}$ , since  $\delta < \min(\gamma, \frac{1}{2})$ .

For all  $\mathbf{n} \in S'_0$  such that  $\mathbf{n} \neq \mathbf{N}/2$ , there are at least  $(|S'_0| - 1)/4!$  statistically independent instances, corresponding to the number of non-intersecting  $\{\mathbf{N} - \mathbf{n}, \mathbf{n} - \mathbf{t}, \mathbf{n} - \mathbf{t} + \mathbf{m}_2, \mathbf{n}\}$

Therefore, (B.12) holds true with probability at most  $p_3^{(|S'_0|-1)/4!}$ .

**Case (iv).** Now consider the combination of the second alternatives in (B.3) and (B.4) that for  $\mathbf{n} \in \mathcal{M}^0 \cap \mathcal{M}^t$

$$\begin{aligned} g(\mathbf{n}) &= e^{i\theta_0 \bar{f}^0(\mathbf{N} - \mathbf{n})} \bar{\mu}^0(\mathbf{N} - \mathbf{n}) / \nu^0(\mathbf{n}) \\ &= e^{i\theta_t \bar{f}^t(\mathbf{N} + 2\mathbf{t} - \mathbf{n} + \mathbf{m}_2)} \bar{\mu}^0(\mathbf{N} + \mathbf{t} - \mathbf{n} + \mathbf{m}_2) / \nu^0(\mathbf{n} - \mathbf{t}) \end{aligned} \tag{B.15}$$

provided that  $\bar{f}^0(\mathbf{N} - \mathbf{n})$  and  $\bar{f}^t(\mathbf{N} + 2\mathbf{t} - \mathbf{n} + \mathbf{m}_2)$  are both zero or nonzero.

Consider any  $\mathbf{n} \in S'_0$  (hence  $\bar{f}^0(\mathbf{N} - \mathbf{n}) \neq 0$ ) and assume  $\bar{f}^t(\mathbf{N} + 2\mathbf{t} - \mathbf{n} + \mathbf{m}_2) \neq 0$ . Otherwise (B.15) is ruled out.

After taking logarithm and rearranging terms for  $\mathbf{n} \in S'_0$  (B.15) becomes

$$\begin{aligned} & \ln \bar{\mu}^0(\mathbf{N} - \mathbf{n}) + \ln \mu^0(\mathbf{n} - \mathbf{t}) - \ln \bar{\mu}^0(\mathbf{N} + \mathbf{t} - \mathbf{n} + \mathbf{m}_2) - \ln \mu^0(\mathbf{n}) \\ &= i\theta_t - i\theta_0 - \ln \bar{f}^0(\mathbf{N} - \mathbf{n}) + \ln \bar{f}^t(\mathbf{N} + 2\mathbf{t} - \mathbf{n} + \mathbf{m}_2) \\ & \quad + \ln \alpha(\mathbf{n}) - \ln \alpha(\mathbf{n} - \mathbf{t}) + i\phi(\mathbf{n}) - i\phi(\mathbf{n} - \mathbf{t}). \end{aligned} \tag{B.16}$$

The imaginary part of the lefthand side of (B.16)

$$\Theta_4 := -\theta(\mathbf{N} - \mathbf{n}) + \theta(\mathbf{n} - \mathbf{t}) + \theta(\mathbf{N} + \mathbf{t} - \mathbf{n} + \mathbf{m}_2) - \theta(\mathbf{n}) \tag{B.17}$$

is the sum of two, three or four independent random variables unless

$$\begin{aligned} \mathbf{N} + \mathbf{t} - \mathbf{n} + \mathbf{m}_2 &= \mathbf{n} \\ \mathbf{N} - \mathbf{n} &= \mathbf{n} - \mathbf{t} \end{aligned}$$

or equivalently

$$\mathbf{m}_2 = 0, \quad \mathbf{n} = \frac{1}{2}(\mathbf{N} + \mathbf{t}).$$

Since  $|S'_0| \geq 2$ , the support of the probability density of  $\Theta_4$  contains  $(-2\gamma\pi, 2\gamma\pi]$ . The same analysis then implies that (B.16) holds true with probability at most  $p_4^{\binom{|S'_0|-1}{4}}$  where

$$p_4 := \max_{a \in \mathbb{R}} \Pr\{\Theta_4 \in (a - 2\delta\pi, a + 2\delta\pi]\} < 1$$

since  $\delta < \min(\gamma, \frac{1}{2})$ .

In summary, ambiguities (i)–(iv) are present with probability at most  $c^s$  and hence the desired result (19) and (20) holds true with probability greater than  $1 - c^s$  where the positive constant  $c < 1$  depends only on  $\delta$  and the probability density function of the mask phase.

### Appendix C. Proof of theorem 3.3

Without loss of generality, we may assume  $\ell_0 = 0$ .

Let  $\mathcal{M}^{\ell(k)}$  denote an adjacent block of  $\mathcal{M}^k$  such that  $f^{\ell(k)}$  and  $f^k$  are  $s$ -connected. When the  $s$ -connected neighbor of  $\mathcal{M}^k$  is not unique, we make an arbitrary selection  $\ell(k)$  such that  $\ell(\ell(k)) = k$ . Let  $L_j = \{f^k, f^{\ell(k)} : k = 0, \dots, j\}$ .

We prove (25) by induction. Suppose that (25) holds for  $k = 0, \dots, j$ . We wish to show that there is another part, say  $f^{j+1} \notin L_j$ , such that (25) holds for  $k = 0, \dots, j, j + 1$ , unless  $j = Q - 1$ . Since  $\{f^k : k = 0, \dots, Q - 1\}$  is  $s$ -connected, at least some  $f^{j+1}$  is  $s$ -connected to, say  $f^l \in L_j$  if  $j < Q - 1$ .

Denote  $S_0 := \mathcal{M}^l \cap \mathcal{M}^{j+1} \cap \text{supp}(f)$ . Applying corollary 2.4 to  $\mathcal{M}^{j+1}$  we have the following alternatives: for some  $\mathbf{m} \in \mathbb{Z}, \theta \in \mathbb{R}$ ,

$$g^{j+1}(\mathbf{n}) = e^{i\theta} f^{j+1}(\mathbf{n} + \mathbf{m}) \mu^{j+1}(\mathbf{n} + \mathbf{m}) / \nu^{j+1}(\mathbf{n})$$

$$\text{or } \text{Twin}(\mathbf{g}^{j+1})(\mathbf{n}) = e^{-i\theta} f^{j+1}(\mathbf{n} + \mathbf{m}) \mu^{j+1}(\mathbf{n} + \mathbf{m}) / \text{Twin}(\nu^{j+1})(\mathbf{n}), \quad \forall \mathbf{n} \in \mathcal{M}^{j+1}. \tag{C.1}$$

Let  $\mathcal{M}^{j+1} = \mathcal{M}^l + \mathbf{t}$  for some shift  $\mathbf{t}$ .

Consider the first alternative for  $\mathbf{n} \in \mathcal{M}^l \cap \mathcal{M}^{j+1}$ :

$$\begin{aligned} e^{i\theta_l f^l(\mathbf{n})} \mu^l(\mathbf{n}) / \nu^l(\mathbf{n}) &= e^{i\theta f^{j+1}(\mathbf{n} + \mathbf{m})} \mu^{j+1}(\mathbf{n} + \mathbf{m}) / \nu^{j+1}(\mathbf{n}) \\ &= e^{i\theta f^{j+1}(\mathbf{n} + \mathbf{m})} \mu^l(\mathbf{n} - \mathbf{t} + \mathbf{m}) / \nu^l(\mathbf{n} - \mathbf{t}) \end{aligned} \tag{C.2}$$

provided that  $f^l(\mathbf{n})$  and  $f^{j+1}(\mathbf{n} + \mathbf{m})$  are both zero or nonzero.

Suppose  $f^l(\mathbf{n}) \cdot f^{j+1}(\mathbf{n} + \mathbf{m}) \neq 0$ . We obtain by taking logarithm on both sides of (C.2) that

$$\begin{aligned} \ln \mu^l(\mathbf{n} - \mathbf{t}) - \ln \mu^l(\mathbf{n} - \mathbf{t} + \mathbf{m}) \\ = i\theta - i\theta_l - \ln f^l(\mathbf{n}) + \ln f^{j+1}(\mathbf{n} + \mathbf{m}) + \ln \alpha(\mathbf{n}) - \ln \alpha(\mathbf{n} - \mathbf{t}) + i\phi(\mathbf{n}) - i\phi(\mathbf{n} - \mathbf{t}) \end{aligned} \tag{C.3}$$

modulo  $i2\pi$ . We want to show that if  $s$  is sufficiently large then (C.3) holds with at most exponentially small probability unless  $\mathbf{m} = 0$ .

Since  $\mathbf{n} \in \mathcal{M}^l \cap \mathcal{M}^{j+1}$  and  $\mathbf{n} + \mathbf{m} \in \mathcal{M}^{j+1}$ ,  $\mathbf{n} - \mathbf{t}$  and  $\mathbf{n} + \mathbf{m} - \mathbf{t}$  belong in  $\mathcal{M}^l$ . Hence the lefthand side of (C.3) is well-defined and has a finite value.

Unless  $\mathbf{m} = 0$ , the imaginary part  $\Theta_1$  of the lefthand side of (C.3)

$$\Theta_1 := \theta(\mathbf{n} - \mathbf{t}) - \theta(\mathbf{n} - \mathbf{t} + \mathbf{m})$$

is the sum of two independent random variables and hence the support set of its probability density contains  $(-2\gamma\pi, 2\gamma\pi]$ .

On the righthand side of (C.3), however, as  $f^l(\mathbf{n})$  and  $f^{j+1}(\mathbf{n} + \mathbf{m})$  are deterministic, the phase fluctuation is determined by  $\phi(\mathbf{n}) - \phi(\mathbf{n} - \mathbf{t})$  which is limited to the interval  $(-2\delta\pi, 2\delta\pi]$  due to MPC( $\gamma$ ). Consequently (C.3) holds true with probability at most

$$p_1 := \max_{a \in \mathbb{R}} \Pr\{\Theta_1 \in (a - 2\delta\pi, a + 2\delta\pi]\} < 1,$$

for each  $\mathbf{n}$ , since  $\delta < \min\{\gamma, 1/2\}$ .

For all  $\mathbf{n} \in S_0$ , there are at least  $|S_0|/2$  statistically independent instances, corresponding to the number of *non-intersecting*  $\{\mathbf{n} - \mathbf{t}, \mathbf{n} + \mathbf{m} - \mathbf{t}\}$ . Therefore (C.3) holds true with probability at most  $p_1^{|S_0|/2}$  unless  $\mathbf{m} = 0$ . On the other hand, for  $\mathbf{m} = 0$ , the desired result (25) for  $k = j + 1$  follows directly from (C.1).

Consider the second alternative in (C.1) and note that

$$\text{Twin}(g^{j+1})(\mathbf{n}) = \bar{g}^{j+1}(\mathbf{N} + 2\mathbf{t}_{j+1} - \mathbf{n}), \quad \text{Twin}(\nu^{j+1})(\mathbf{n}) = \bar{\nu}^{j+1}(\mathbf{N} + 2\mathbf{t}_{j+1} - \mathbf{n}).$$

Rewriting the second alternative we obtain for  $\mathbf{n} \in \mathcal{M}^l \cap \mathcal{M}^{j+1}$

$$\begin{aligned} e^{i\theta_l f^l(\mathbf{n})} \mu^l(\mathbf{n}) / \nu^l(\mathbf{n}) \\ = e^{i\theta \bar{f}^{j+1}(\mathbf{N} + 2\mathbf{t}_{j+1} - \mathbf{n} + \mathbf{m})} \bar{\mu}^{j+1}(\mathbf{N} + 2\mathbf{t}_{j+1} - \mathbf{n} + \mathbf{m}) / \nu^{j+1}(\mathbf{n}), \\ = e^{i\theta \bar{f}^{j+1}(\mathbf{N} + 2\mathbf{t}_{j+1} - \mathbf{n} + \mathbf{m})} \bar{\mu}^l(\mathbf{N} + 2\mathbf{t}_l - \mathbf{t} - \mathbf{n} + \mathbf{m}) / \nu^l(\mathbf{n} - \mathbf{t}), \end{aligned} \tag{C.4}$$

provided that  $f^l(\mathbf{n})$  and  $\bar{f}^{j+1}(\mathbf{N} + 2\mathbf{t}_{j+1} - \mathbf{n} + \mathbf{m})$  are both zero or nonzero.

Consider any  $\mathbf{n} \in S_0$  (hence  $f^l(\mathbf{n}) \neq 0$ ) and assume  $\bar{f}^{j+1}(\mathbf{N} + 2\mathbf{t}_{j+1} - \mathbf{n} + \mathbf{m}) \neq 0$ . Otherwise (C.4) is false and can be ruled out.

Taking logarithm and rearranging terms in (C.4) we have

$$\begin{aligned} \ln \mu^l(\mathbf{n} - \mathbf{t}) - \ln \bar{\mu}^l(\mathbf{N} + 2\mathbf{t}_l - \mathbf{t} - \mathbf{n} + \mathbf{m}) \\ = i\theta - i\theta_l - \ln f^l(\mathbf{n}) + \ln \bar{f}^{j+1}(\mathbf{N} + 2\mathbf{t}_{j+1} - \mathbf{n} + \mathbf{m}) + \ln \alpha(\mathbf{n}) - \ln \alpha(\mathbf{n} - \mathbf{t}) \\ + i\phi(\mathbf{n}) - i\phi(\mathbf{n} - \mathbf{t}). \end{aligned} \tag{C.5}$$

The imaginary parts of the lefthand side of (C.5)

$$\Theta_2 := \theta(\mathbf{n} - \mathbf{t}) + \theta(\mathbf{N} + 2\mathbf{t}_l - \mathbf{t} - \mathbf{n} + \mathbf{m})$$

is the sum of two independent random variables unless

$$\mathbf{n} = \mathbf{t}_l + \frac{1}{2}(\mathbf{N} + \mathbf{m})$$

in which case  $\Theta_2 = 2\theta(\mathbf{n} - \mathbf{t})$  is not a sum of two independent random variables. Hence the support of the probability density function of  $\Theta_2$  contains  $(-2\gamma\pi, 2\gamma\pi]$ . By the same argument as above, (C.5) holds true with probability at most  $p_2^{|S_0|/2}$  where

$$p_2 := \max_{a \in \mathbb{R}} \Pr\{\Theta_2 \in (a - 2\delta\pi, a + 2\delta\pi]\} < 1$$

since  $\delta < \min(\gamma, \frac{1}{2})$ .

Combining the analysis of the two alternatives, (25) fails for  $k = j + 1$  with probability at most  $p_1^{|S_0|/2} + p_2^{|S_0|/2} \leq 2p^{|S_0|/2}$  conditioned on the event that (25) holds true for  $k = 0, \dots, j$  where  $p$  is as given in (23). Therefore, the desired result (25) holds with probability at least  $1 - 2Qp^{|S_0|/2}$  after subtracting the failure probability for each additional block.

## ORCID iDs

Albert Fannjiang  <https://orcid.org/0000-0003-3150-7392>

Pengwen Chen  <https://orcid.org/0000-0002-4586-0552>

## References

- [1] Almore P F and Hanson S G 2008 Random phase plate for wavefront sensing via phase retrieval and a volume speckle field *Appl. Opt.* **47** 2979–87
- [2] Almore P F, Pedrini G, Gundu P N, Osten W and Hanson S G 2011 Enhanced wavefront reconstruction by random phase modulation with a phase diffuser *Opt. Laser Eng.* **49** 252–7
- [3] Bodin A, Dèbes P and Najib S 2009 Irreducibility of hypersurfaces *Commun. Algorithms* **37** 1884–900
- [4] Bräuer R, Wojak U, Wyrowski F and Bryngdahl O 1991 Digital diffusers for optical holography *Opt. Lett.* **16** 1427–9
- [5] Bunk O, Dierolf M, Kynde S, Johnson I, Marti O and Pfeiffer F 2008 Influence of the overlap parameter on the convergence of the ptychographical iterative engine *Ultramicroscopy* **108** 481–7
- [6] Chapman H N and Nugent K A 2010 Coherent lensless x-ray imaging *Nat. Photon.* **4** 833–9
- [7] Chen P and Fannjiang A 2008 Coded-aperture ptychography: uniqueness and reconstruction *Inverse Problems* **34** 025003
- [8] Dierolf M, Menzel A, Thibault P, Schneider P, Kewish C M, Wepf R, Bunk O and Pfeiffer F 2010 Ptychographic x-ray computed tomography at the nanoscale *Nature* **467** 436–9
- [9] Dierolf M, Thibault P, Menzel A, Kewish C, Jefimovs K, Schlichting I, Kong K, Bunk O and Pfeiffer F 2010 Ptychographic coherent diffractive imaging of weakly scattering specimens *New J. Phys.* **12** 035017
- [10] Egami R, Horisaki R, Tian L and Tanida J 2016 Relaxation of mask design for single-shot phase imaging with a coded aperture *Appl. Opt.* **55** 1830–7
- [11] Fannjiang A 2011 Exact localization and superresolution with noisy data and random illumination *Inverse Problems* **27** 065012
- [12] Fannjiang A 2012 Absolute uniqueness of phase retrieval with random illumination *Inverse Problems* **28** 075008
- [13] Fannjiang A 2019 Raster scan pathology and the cure *SIAM Multiscale Mod. Simul.* **17** 973–95
- [14] Fannjiang A and Chen P 2018 Blind ptychography: uniqueness & ambiguities (arXiv:1806.02674)

- [15] Fannjiang A and Liao W 2012 Phase retrieval with random phase illumination *J. Opt. Soc. A* **29** 1847–59
- [16] Fannjiang A and Liao W 2013 Fourier phasing with phase-uncertain mask *Inverse Problems* **29** 125001
- [17] Fannjiang A and Zhang Z 2019 Fixed point analysis of Douglas–Rachford splitting for ptychography and phase retrieval (arXiv:1909.08600)
- [18] Faulkner H M L and Rodenburg J M 2004 Movable aperture lensless transmission microscopy: a novel phase retrieval algorithm *Phys. Rev. Lett.* **93** 023903
- [19] Gao S, Wang P, Zhang F, Martinez G T, Nellist P D, Pan X and Kirkland A I 2017 Electron ptychographic microscopy for three-dimensional imaging *Nat. Commun.* **18** 163
- [20] Guizar-Sicairos M and Fienup J R 2008 Phase retrieval with transverse translation diversity: a nonlinear optimization approach *Opt. Express* **16** 7264–78
- [21] Guo K, Dong S, Nanda P and Zheng G 2015 Optimization of sampling pattern and the design of Fourier ptychographic illuminator *Opt. Express* **23** 6171–80
- [22] Hayes M 1982 The reconstruction of a multidimensional sequence from the phase or magnitude of its Fourier transform *IEEE Trans. Acoust. Speech Signal Process.* **30** 140–54
- [23] Hesse R, Luke D R, Sabach S and Tam M K 2015 Proximal heterogeneous block implicit-explicit method and application to blind ptychographic diffraction imaging *SIAM J. Imag. Sci.* **8** 426–57
- [24] Huang X, Yang H, Harder R, Hwu Y, Robinson I K and Chu Y S 2014 Optimization of overlap uniformness for ptychography *Opt. Express* **22** 12634–44
- [25] Hoppe W 1969 Beugung im inhomogenen Primrstrahlwellenfeld. I. Prinzip einer Phasenmessung von Elektronenbeugungsinterferenzen *Acta Crystallogr. A* **25** 495
- [26] Hoppe W 1969 Beugung im inhomogenen Primrstrahlwellenfeld. III. Amplituden- und Phasenbestimmung bei unperiodischen Objekten *Acta Crystallogr. A* **25** 508
- [27] Horisaki R, Egami R and Tanida J 2016 Single-shot phase imaging with randomized light (SPIRaL) *Opt. Express* **24** 3765–73
- [28] Hunt J, Driscoll T, Mrozack A, Lipworth G, Reynolds M, Brady D and Smith D R 2013 Metamaterial apertures for computational imaging *Science* **339** 310–3
- [29] Jiang Y *et al* 2018 Electron ptychography of 2D materials to deep sub-angstrom resolution *Nature* **559** 343–9
- [30] Lipworth G, Mrozack A, Hunt J, Marks D L, Driscoll T and Brady D 2013 Metamaterial apertures for coherent computational imaging on the physical layer *J. Opt. Soc. Am. A* **30** 1603–12
- [31] Maiden A, Johnson D and Li P 2017 Further improvements to the ptychographical iterative engine *Optica* **4** 736–45
- [32] Maiden A M, Morrison G R, Kaulich B, Gianoncelli A and Rodenburg J M 2013 Soft x-ray spectromicroscopy using ptychography with randomly phased illumination *Nat. Commun.* **4** 1669
- [33] Maiden A M and Rodenburg J M 2009 An improved ptychographical phase retrieval algorithm for diffractive imaging *Ultramicroscopy* **109** 1256–62
- [34] Marchesini S, Krishnan H, Daurer B J, Shapiro D A, Perciano T, Sethian J A and Maia F R 2016 SHARP: a distributed GPU-based ptychographic solver *J. Appl. Crystallogr.* **49** 1245–52
- [35] Miao J, Sayre D and Chapman H N 1998 Phase retrieval from the magnitude of the Fourier transforms of nonperiodic objects *J. Opt. Soc. Am. A* **15** 1662–9
- [36] Nashed Y S G, Vine D J, Peterka T, Deng J, Ross R and Jacobsen C 2014 Parallel ptychographic reconstruction *Opt. Express* **22** 32082–97
- [37] Nellist P D, McCallum B C and Rodenburg J M 1995 Resolution beyond the information limit in transmission electron microscopy *Nature* **374** 630–2
- [38] Nellist P D and Rodenburg J M 1998 Electron ptychography. I. Experimental demonstration beyond the conventional resolution limits *Acta Crystallogr. A* **54** 49–60
- [39] Nugent K A 2010 Coherent methods in the x-ray sciences *Adv. Phys.* **59** 1–99
- [40] Ou X, Zheng G and Yang C 2014 Embedded pupil function recovery for Fourier ptychographic microscopy *Opt. Express* **22** 4960–72
- [41] Pan A, Zhang Y, Wen K, Zhou M, Min J, Lei M and Yao B 2018 Subwavelength resolution Fourier ptychography with hemispherical digital condensers *Opt. Express* **26** 23119–31
- [42] Peng X, Ruane G J, Quadrelli M B and Swartzlander G A 2017 Randomized apertures: high resolution imaging in far field *Opt. Express* **25** 296187
- [43] Pfeiffer F 2017 X-ray ptychography *Nat. Photon.* **12** 9–17

- [44] Plamann T and Rodenburg J M 1998 Electron ptychography. II. Theory of three-dimensional propagation effects *Acta Crystallogr. A* **54** 61–73
- [45] Rodenburg J M 2008 Ptychography and related diffractive imaging methods *Adv. Imaging Electron Phys.* **150** 87–184
- [46] Rodenburg J M and Faulkner H M L 2004 A phase retrieval algorithm for shifting illumination *Appl. Phys. Lett.* **85** 4795
- [47] Seaberg M H, d’Aspremont A and Turner J J 2015 Coherent diffractive imaging using randomly coded masks *Appl. Phys. Lett.* **107** 231103
- [48] Sidorenko P, Lahav O, Avnat Z and Cohen O 2016 Ptychographic reconstruction algorithm for frequency-resolved optical gating: super-resolution and supreme robustness *Optica* **3** 1320–30
- [49] Stockmar M, Cloetens P, Zanette I, Enders B, Dierolf M, Pfeiffer F and Thibault P 2013 Near-field ptychography: phase retrieval for inline holography using a structured illumination *Sci. Rep.* **3** 1927
- [50] Sylman D, Micó V, Garca J and Zalevsky Z 2010 Random angular coding for superresolved imaging *Appl. Opt.* **49** 4874–82
- [51] Thibault P, Dierolf M, Bunk O, Menzel A and Pfeiffer F 2009 Probe retrieval in ptychographic coherent diffractive imaging *Ultramicroscopy* **109** 338–43
- [52] Thibault P, Dierolf M, Menzel A, Bunk O, David C and Pfeiffer F 2008 High-resolution scanning x-ray diffraction microscopy *Science* **321** 379–82
- [53] Thibault P and Guizar-Sicairos M 2012 Maximum-likelihood refinement for coherent diffractive imaging *New J. Phys.* **14** 063004
- [54] Valzania L, Feurer T, Zolliker P and Hack E 2018 Terahertz ptychography *Opt. Lett.* **43** 543–6
- [55] Watts C M, Shrekenhamer D, Montoya J, Lipworth G, Hunt J, Sleasman T, Krishna S, Smith D R and Padilla W J 2014 Terahertz compressive imaging with metamaterial spatial light modulators *Nat. Photon.* **8** 605–9
- [56] Yeh L, Dong J, Zhong J, Tian L, Chen M, Tang G, Soltanolkotabi M and Waller L 2015 Experimental robustness of Fourier ptychography phase retrieval algorithms *Opt. Express* **23** 33214–40
- [57] Zhang F, Chen B, Morrison G R, Vila-Comamala J, Guizar-Sicairos M and Robinson I K 2016 Phase retrieval by coherent modulation imaging *Nat. Commun.* **7** 13367
- [58] Zhang F, Pedrini G and Osten W 2007 Phase retrieval of arbitrary complex-valued fields through aperture-plane modulation *Phys. Rev. A* **75** 043805
- [59] Zhang X, Jiang J, Xiangli B and Arce G R 2015 Spread spectrum phase modulation for coherent x-ray diffraction imaging *Opt. Express* **23** 25034–47
- [60] Zheng G, Horstmeyer R and Yang C 2013 Wide-field, high-resolution Fourier ptychographic microscopy *Nat. Photon.* **7** 739–45